Heliyon 8 (2022) e10943

Contents lists available at ScienceDirect

Heliyon

journal homepage: www.cell.com/heliyon

Review article

Ultrafast growth of carbon nanotubes using microwave irradiation: characterization and its potential applications

Paramjeet Baghel, Anil Kumar Sakhiya, Priyanka Kaushal *

Centre for Rural Development and Technology, Indian Institute of Technology- Delhi, New Delhi 110016, India

HIGHLIGHTS

- Synthesis of carbon nanotubes using different methods.
- Microwave irradiation techniques are used for the growth of CNTs.
- Current challenge and future aspects of CNTs growth.
- Detailed characterization and application of CNTs.

GRAPHICAL ABSTRACT

ARTICLE INFO

Keywords:
Carbon nanotubes
Synthesis methods
Microwave irradiation
CNTs characterization
CNTs applications

ABSTRACT

Carbon nanotubes (CNTs) have been studied for more than twenty-five years due to their distinguishing features such as high tensile strength, high elastic module, high surface area, high thermal and electrical conductivity, making them ideal for a variety of applications. Nanotechnology and nanoscience researchers are working to develop CNTs with appropriate properties for possible future applications. New methodologies for their synthesis are clearly needed to be developed and refined. In this research, the authors look at the history and the recent developments of carbon nanotubes synthesis methods for CNTs, such as arc discharge, laser ablation, chemical vapour deposition and microwave irradiation. New immerging methods like microwave irradiation for the growth of CNTs and their composite was extensively reviewed. Low temperature and ultrafast growth of CNT through microwave irradiation technique were examined and discussed. In addition, all the techniques used for the CNTs characterization were also briefly discussed. Special attention was dedicated to the application of CNTs. This review has extensively explored future applications in the biomedical sector, industrial water purifications, CNTs composites, energy and storage devices.

1. Introduction

The popularity of carbon nanotubes (CNTs) among scientists was increased exponentially in the last three decades. Initially, in 1991, Sumio Iijima developed a carbon filament which having a nanometre range diameter [1]. This carbon filament is known as a carbon nanotube. It is just the rolled-up sheets of graphene with sp^2 hybridization. In the next 2 years, Iijima and Ichihashi [2] and Bethune et al. developed the single-wall carbon nanotubes (SWCNT) [3]. Carbon nanotubes can be a double shell (DWCNT) or multi-shell (MWCNT) with a hollow cylindrical structure. The variation in shell formation depends on the method adopted to synthesize CNTs. Synthesized CNTs have a

* Corresponding author.
E-mail address: priyankak@iitd.ac.in (P. Kaushal).

https://doi.org/10.1016/j.heliyon.2022.e10943
Received 7 April 2022; Received in revised form 27 June 2022; Accepted 29 September 2022

length of a few microns, and their diameter varies in the range of nanometres (10–100 nm). On the basis of curvature along its circumference and the concept of chiral vector, CNTs divided into three categories: chiral (n, m), zigzag (n, 0) and armchair (n, n) [4]. These categories make CNTs conducting (metallic) or semiconducting and open to a wide range of electronic applications. Individual categories of CNTs have their unique characteristic, which can be used in various applications. CNTs have a wide range of applications in, such as nano composites of metal oxides, transparent conducting films, energy storage devices, super capacitors, field emit transistors, semiconductors, battery electrodes, high strength fibres, biomedical applications, sensors, biosensors, nano sensors, paint and coating, microwave absorption and water treatment [5, 6, 7, 8, 9, 10].

CNTs are gaining popularity in the commercial industry around the world as a result of their emerging applications. Meet the high demand for CNTs in various applications forced scientists to produce the CNTs in bulk amounts. This leads scientists to develop the new CNTs synthesis methods. To produce defect-free CNTs in a large amount is a bit difficult. At present, different techniques like arc-discharge, laser ablation, Chemical vapour deposition (CVD) has been used for synthesis. These techniques mainly used the feed as ethane, ethylene, carbon monoxide, methane, benzene, xylene, and graphite rods for synthesis. SWCNTs are formed by linear hydrocarbons, whereas cyclic hydrocarbons form MWCNTs. Arc discharge, laser ablation, and CVD operate at very high temperatures (>1000 °C) [4]. Furthermore, purification of CNTs from soot and unwanted catalyst is required after synthesis. CNTs are synthesized in small quantities (in mg), which raises the cost of CNTs. As a result, these processes become more expensive for high-quality and large-quantity CNTs. Purifying, manipulating, and assembling CNTs for creating nanotube structures for practical applications is tough with existing procedures. Thus, various new advancements in conventional approaches and new ways have been discovered in order to grow a high-quality and large-scale production of CNTs. Other methods like catalytic chemical vapor deposition, diffusion flame synthesis, electrolysis, heat treatment of polymers, and low-temperature solid pyrolysis were also developed to grow the CNTs. To minimise the cost of the process, scientists developed techniques which can be operated at low temperatures. Advancements in CVD and microwave irradiation techniques have resulted in a new process for producing bulk CNTs with lower impurity levels.

This paper presents a brief overview of conventional techniques such as CVD, arc-discharge, and laser ablation as well as a thorough examination of a new emergent microwave irradiation methodology for the production of CNTs. Different methods for characterising CNTs were also discussed. In this review, future applications of CNTs in various fields like energy storage devices, biomedical, sensors, CNTs metal oxide composites, and industrial water remediation were all discussed.

2. Literature review methodology

The literature selected for the review has been selected by considering criteria like chronology, keywords, publication type and publication content. The literature was identified by a web of science database. The keywords were used separately and in different combinations. Main keywords used were carbon nanotube, synthesis, microwave irradiation, characterization, and application. A total of 163 articles were selected from the database, including the research articles, book chapters, technical papers, conference papers, and review papers. The network visualization map of articles with the help of VOS viewer software (version 1.6.18) was created, as illustrated in Figure 1(a). The weightage of the references in this review for the years 2008–2022 (73.26%), 1996 to 2007 (19.20%) and before 1996 (7.54%). The year-wise distribution of the references is presented in Figure 1(b). The primary literature focused on CNT growth from microwave irradiation and its potential application in various fields. This review covers the past to present research and development trends in the growth and potential of the CNTs.

3. Different synthesis techniques for CNTs

Initially, CNTs were synthesized in 1991 by Iijima in Japan [1]. For high quality and quantity CNTs, several methods have been developed. Frequently, chemical vapour deposition (CVD), laser ablation, and arc discharge methods are mainly applied, whereas recently, the microwave irradiation technique has been used for high purity CNTs [11, 12, 13]. The general overview of these procedures and their products is shown in Table 1. Arc-discharge and CVD methods were conducted under vacuum, and atmospheric pressure conditions, whereas laser ablation and microwave methods, can be done in only vacuum with controlled inert gases [14]. Microwave irradiation, CVD, and carbon arc discharge have high production rates. Recently, some researchers used biochar as precursor used to synthesize the CNTs through microwave irradiation [12, 13]. Biochar is easily produced by pyrolysis of biomass at cheaper rate [15, 16, 17]. For cheaper volume CNTs production, new methods and eco-friendly precursors are still under research. New techniques for CNTs manufacturing may be results in large-scale and more affordable production [18]. For example, waste plastic, waste biomass, biochar and recycled car tires as carbon sources have been used to produce low-cost CNTs [12, 19].

3.1. Arc-discharge

This was the first method used to synthesize CNTs by Iijima [20]. The experimental apparatus and condition are almost similar to the fullerene production. This method produced CNTs at high temperatures (above 1700 °C) from the graphite electrode. This method involves two graphite electrodes placed apart 1 mm from each other in the reaction chamber, as shown in Figure 2. One is an anode, and the other is a cathode having 6mm and 9mm diameter, respectively [21]. The reaction takes place under a mixture of an Ar/H_2 in a high-pressure chamber. Approximately 50–100 A current is applied with a potential difference of 18 V over the electrodes [22]. A plasma is formed due to discharge when the opposite electrodes are brought together. The temperature is very high in the chamber by which carbon evaporates from electrodes. The soot-like material with CNTs is deposited on the larger electrode (cathode electrode) by condensation. SWCNTs were produced with a diameter of 2 nm–7 nm when an anode electrode is doped with a metal catalyst such as Iron (Fe), cobalt (Co), nickel (Ni), Gadolinium (Gd) or Yttrium (Y) [23, 24, 25, 26]. Approximately 1–3 nm inner diameter and 2–25 nm outer diameter MWCNTs deposited on the negative electrode were observed [1, 27]. This method can be used for the large production of SWCNTs/MWCNTs. However, encapsulation of metal catalysts (Fe, Co, Ni) in the CNTs would introduce further purification steps, which leads to the limited yield of CNTs.

3.2. Chemical vapour deposition (CVD)

CVD is the most widely used technique for the large-scale production of CNTs. This technique involved the growth of CNTs on catalysts made by metal nanoparticles of Fe, Co, Ni, and Mo in reducing the environment of hydrogen, argon and ammonia gas. In addition, some scientists also used the Pt, Cu, Ag, and Au metal catalyst. These catalysts play a vital role in the synthesis of CNTs. A layer of Al_2O_3, MgO, and SiO_2 is used, called a substrate, to support the metal catalyst. Metal catalyst and substrate bind together with the help of van Der Waals forces. Light hydrocarbon gases such as CH_4 and C_2H_2 are used as a precursor of carbon sources for the growth of CNT. The schematic diagram of the CVD method is shown in Figure 3(a). Sometimes liquid benzene, alcohol and solid form of camphor are also used as a carbon source [21]. The growth mechanism of CNTs on catalyst has taken place in the temperature range of 600–1100 °C and is shown in Figure 3(b-c). With the growth of CNT at a lower temperature, it is easy to control the parameters responsible for high CNTs production. It also gives the option of selective growth of CNTs on a substrate surface. Most of the electronic sensors, devices, and circuits

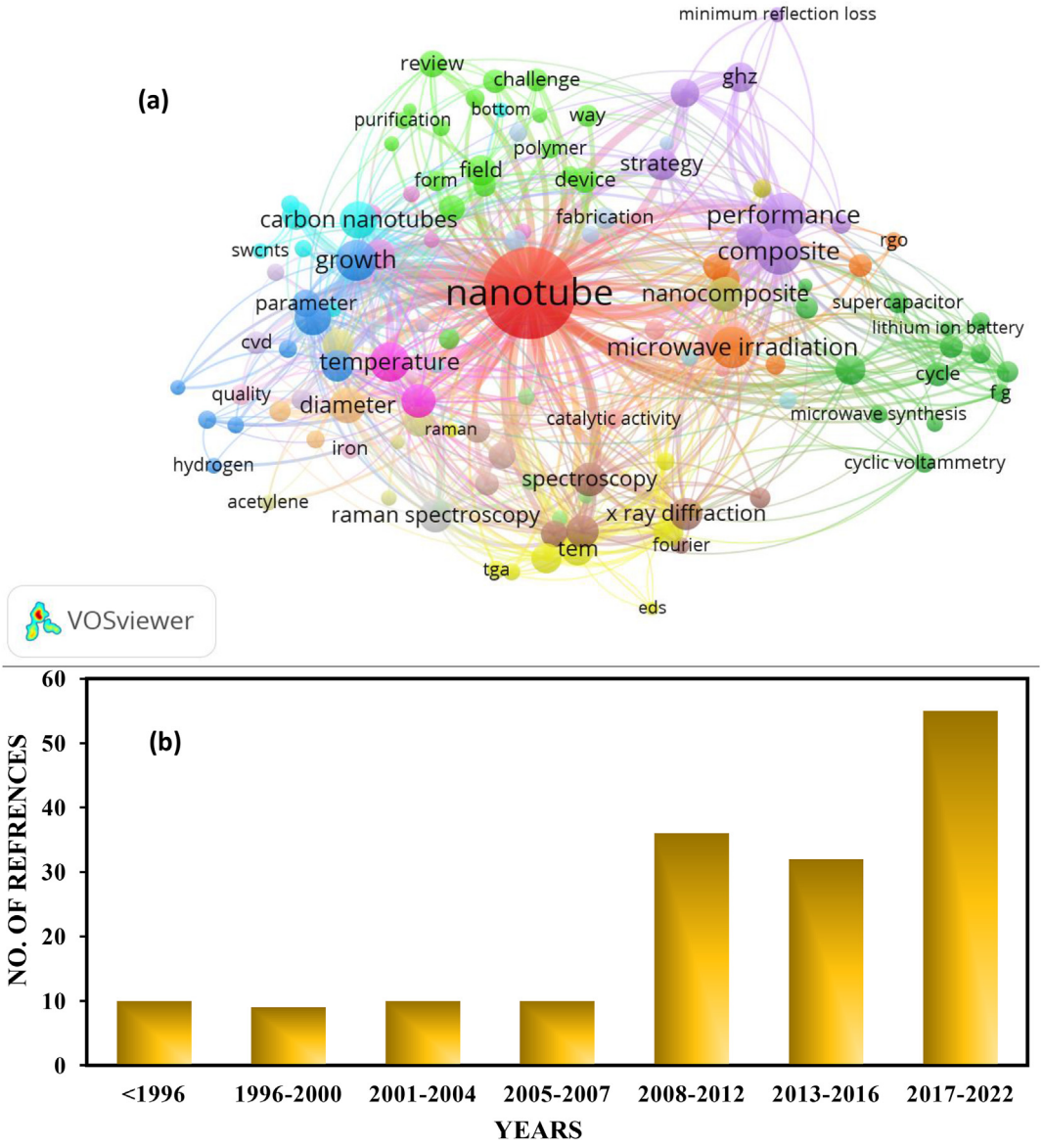

Figure 1. (a) Network visualization map of the synthesis, characterization and application of carbon nanotubes. (b) Year-wise distribution of selected articles for literature review.

Table 1. The general overview of procedure and their products are shown.

Synthesis Methods	Catalysts Used	CNTs Yield (%)	SWCNTs	MWCNTs	Advantages	Disadvantages	Reference
CVD	Fe, Ni, Co Support- Al_2O_3	20–100	Length: nm to cm OD:0.6–4nm	Length: nm to cm OD: 10–240 nm	• Diameter of CNTs is controllable • long CNTs produced	• High Impurities • Defects in CNTs	[59]
Arc Discharge	Anode is doped with Co, Ni, Fe	30–90	Length: OD: 0.6–1.4	Length: ~ 20 μm ID: 1–3 nm OD: ~ 10 nm	• Easy production of CNTs • Produced without catalyst • Open air synthesis possible	• Produced CNTs are in aggregates and bundles • Co-production of fullerene occur • Further Purification required due to crystalline and amorphous carbon	[22]
Laser Ablation	Metal-doped carbon source Ni, Co, Pt., Rh, [NiCo]	Up to 70	Length: 5–20μm OD: 1–2nm	Length: ~ 20 μm ID: 1–3 nm OD: ~ 10 nm	• High quality CNTs produced • Size is controllable	• CNTs produced in bundles and robes • Low amount of CNTs produced • Need purification of amorphous carbon and metal catalyst	[32, 35]
Microwave Irradiation	Ferrocene	-	-	OD:17-100	• Less energy intensive • Easy and CNTs produced in Seconds	• Irregularities in shape • Metal encapsulated in CNTs	[12]

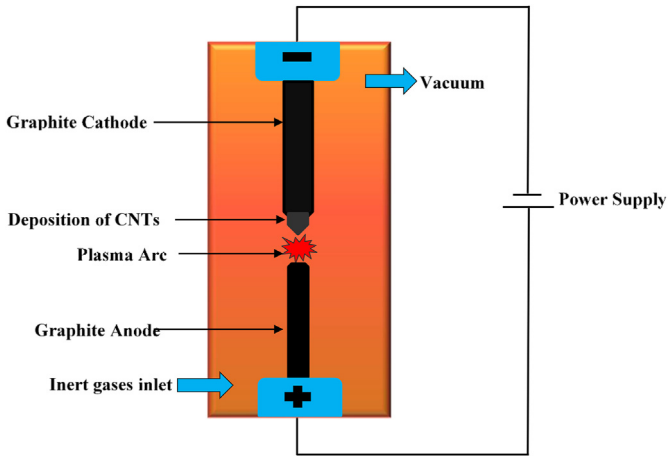

Figure 2. - Arc-discharge setup.

required flexible CNTs, and it was synthesized at low temperature (25–500 °C).

After the discovery of CNTs, the CVD method was readily adopted for bulk production. Different upgradations take place in CVD methods such as plasma-enhanced CVD, thermal CVD, photothermal CVD, aerosol-assisted CVD, alcohol catalytic CVD, aerogel-supported CVD, laser-assisted CVD, and remote plasma CVD. The most widely used techniques for the synthesis of CNTs are TCVD and PECVD.

On the basis of hydrocarbon and catalysts, the growth mechanism is decided, such as vapour-solid-solid (VSS) and vapour-liquid-solid (VLS). Most of the studies used VLS as a growth mechanism. In VLS, the catalyst remains in a liquid state, whereas hydrocarbons are adsorbed on metal catalysts, and decomposition occurs. The growth of CNTs occurs because the carbon forms a liquid eutectic by dissolving into the particle [28, 29]. On the other side, VSS have solid catalyst [30].

Zhang et al. reported that the tubular and multi-wall CNTs were developed from pine nut shell biochar using microwave irradiation in CVD [31]. The methane as a carbon source and Ni as a catalyst was used for CNT development. High quality and quantity CNTs were synthesized at 600 °C with a heating rate of 200 °C/min and 60 min residence time. They highlighted the role of microwave heating and Ni catalyst in the growth of CNTs. In addition, higher carbon order of CNTs was achieved due to increment in aromatic rings cluster during microwave heating.

3.3. Laser ablation

This technique is similar to arc discharge. Both the methods involved the vaporisation of graphite and the condensation of carbon forms CNTs. However, a continuous laser beam, or a pulsed laser ablation, is employed to heat the targeted graphite specimen, as displayed in Figure 4, whereas arc-discharge uses the high voltage current. In a quartz tube furnace, the high-intensity laser irradiation evaporates the carbon atoms of graphite under an inert atmosphere (He, Ar, and N_2) at 1200 °C. The evaporated carbon atom condenses over the cooler surface of the reactor, and CNTs are formed [32, 33, 34]. MWCNTs with 1nm–2nm

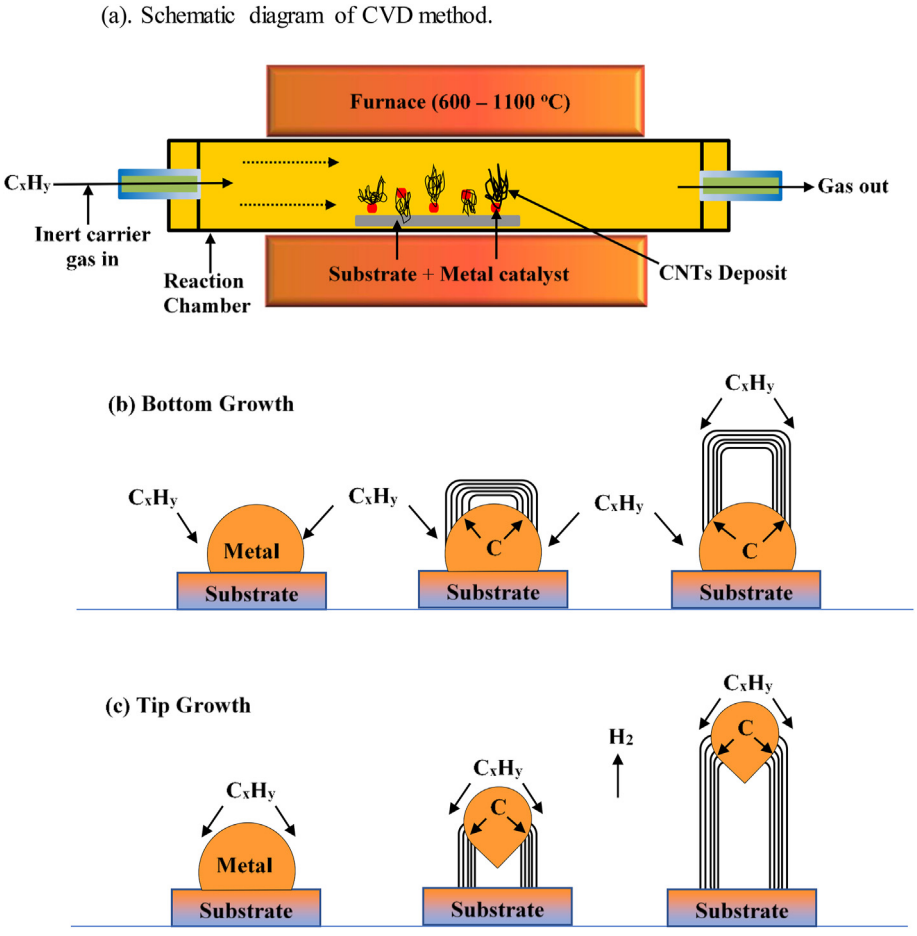

Figure 3. (a). Schematic diagram of CVD method. Growth mechanism of CNTs (b) Bottom growth (c) Tip growth (Reproduced from Ref. [21] copyright 2004, with permission from Elsevier.).

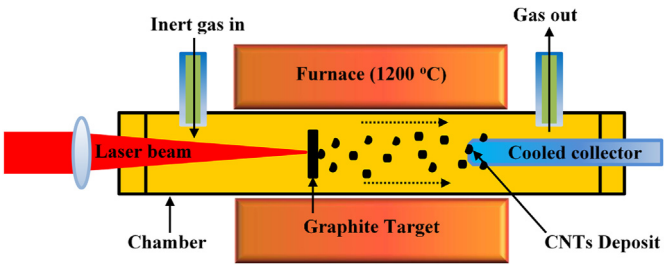

Figure 4. Laser ablation setup.

inner diameter and 10nm outer diameter are produced using both the pure graphite electrodes [35]. When targeted graphite is doped with the metal catalyst Fe, Co or Ni, SWCNTs were made. The quality and quantity of CNTs depend on the following parameters: reaction temperature, inert gases, the pressure inside the tube and laser properties. Due to fewer impurities in CNTs, this technique is advantageous over the arc-discharge method, and it requires less intense purification steps after growth.

3.4. Microwave irradiation

Asnawi et al. studied CNT development from rice husk using microwave oven induced plasma irradiation [36]. They carried out a reaction between ferrocene as a catalyst and ~20 μm size rice husk in a microwave oven of 600 W power and 2.45 GHz frequency (Samsung M539 MAN200405W). The process was conducted at a temperature of 750 °C and 40-minute residence time. During the growth of CNT, quartz tube pressure dropped from 3 to 1 mbar. They produced a twisted and web-like network of CNTs, as shown in Figure 5 and the ratio of (I_D/I_G) bandgap 1.013 was calculated for the synthesized nanomaterials. The D and G band intensities (I_D/I_G) ratio indicate lower quality sp^2 carbon structures.

Hildago-Oporto et al. investigated the development of CNTs using microwave irradiation. They used the biochar of wheat straw, oats hull, rapeseed cake and hazelnut hull as a precursor material to synthesize CNTs [12]. They mixed the biochar produced at 400 and 600 °C with ferrocene. The synthesis occurs at 80 °C, 17 psi pressure and 200 W power, 2.45 GHz frequency microwave reactor (CEM Discover microwave reactor) for 5 min. It was observed that the biochar produced at 600 °C resulted in a high concentration of CNTs as compared to those produced at 400 °C. It might be due to the high carbon content in biochar produced at a higher temperature. The produced CNTs have a diameter

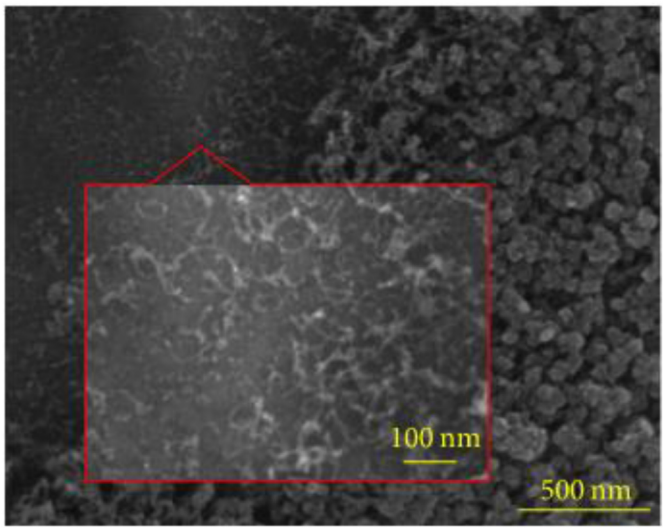

Figure 5. CNTs are twisted and intertwined in web like network (Reproduced from Ref. [36] Copyright, 2018 Muhammad Asnawi et al.).

in a range of 17–100 nm, as shown in Figure 6. CNTs derived from Hazelnut hull and wheat straw have less diameter and better quality.

Zhan et al. demonstrated the ultrafast growth of CNTs in 20–40 s [37]. The CNTs growth was achieved in a domestic microwave oven with a ferrocene catalyst at room temperature. For precursor material, copper wire, iron wire, molybdenum wire and steel fibre were used. The diameter of produced CNTs ranges between 10 to 160 nm, the diameter of Cu made CNTs ranges from 30 – 40 nm, whereas Mo made CNTs have the range of 10–120 nm. CNTs made from iron wire and steel fibre have a small diameter of 0–60 nm.

Kumar et al. reported the synthesis of palladium-graphene oxide-based CNTs (PD-CNTs-rGO) and its enhanced electron field emission studies [38]. They prepared the composite in 1.5 min at 810 W powered domestic microwave oven (Consul-CMW30AB). PD-CNTs-rGO composite shows high field emission performance with an enhanced factor of 4230 due to proper contact of CNT and graphene oxide.

Algadri et al. performed low-cost, low temperature, and fast-growth CNTs using the microwave irradiation technique [39]. CNTs growth was achieved in a domestic microwave oven operating at 2.54 GHz with 800 W in 5s. They used graphite as a carbon source and ferrocene as a catalyst. The produced CNTs have a diameter of 44–79 nm. They investigated the effect of graphite to ferrocene mixture ratio using Raman spectroscopy, Transmission electron microscopy (TEM), Scanning electron microscopy (SEM) and X-ray Diffraction (XRD). They reported that the 70:30 ratio of graphite/ferrocene mixture gives a better yield than other ratios. This ratio also indicates better crystallinity and better quality CNTs. However, Fe metal encapsulated inside the CNTs decreases the quality of CNTs.

Bajpai and Wagner showed the synthesis of CNTs within 5 s in ambient conditions using the microwave irradiation technique [40]. They used carbon fibre and graphite as carbon sources for synthesis and ferrocene as a catalyst. Microwave heating was conducted in a commercial microwave oven operating (DEC18E2, ACP) at 2.45 GHz with 1800 W power. They achieved the 82 % carbon conversion efficiency and yield of CNTs around 26 % with 5 % variation at 100 % MW power. They reported the average diameter and length of CNTs were 17 ± 10 nm and 1.4± 0.7 μm, respectively. In addition, the quality of CNT is decreased due to the capillary effect, which causes the encapsulation of *Fe nanoparticles* in CNTs, as shown in Figure 7.

Kang et al. studied the synthesis of the hybrid structure of CNTs with the help of ice templating and domestic microwave [41]. They adopted the three-dimensional (3D) microporous, nitrogen-doped reduced graphene oxide (NG) and ferrocene as a catalyst to prepare the branched CNTs on NG. They achieved the synthesis in 150 s, which was noted by CNT/NG-Fe, and without doping of nitrogen on graphene oxide was noted as CNT/G-Fe as shown in Figure 8.

They reported the electrochemical performances of these hybrids and compared the discharge capacity of the 3D CNT/NG-Fe, CNT/G-Fe and NG. They found a much higher discharge capacity of 3D CNT/NG-Fe compared to others. They also reported the retention capacity of 52 % of the initial capacity, which corresponds to the discharge capacity of 947 mAh g^{-1} when the rate upsurges 100 to 1000 mAh g^{-1}. Moreover, columbic efficiency of >98.5 % was achieved after 130 cycles at 100 mAh g^{-1}, which equals to 1020 mAh g^{-1} discharge capacity. Figure 9 (a) shows the electrochemical behaviour of the CNT/NG-Fe, and Figure 9(b) shows cycle stability, columbic efficiency of different CNTs at 100 mAh g^{-1}.

Omoriyekomwan et al. highlighted the direct growth of CNTs from biomass component cellulose at a low temperature of 600 °C using the microwave pyrolysis technique [42]. They used the palm kernel shell (PKS) and separated the components cellulose and lignin using two isolate methods, i.e., Alkaline-acid (ALAC) and Formic acid/acetic acid (FAAC). They reported that CNTs growth was promoted by detecting monosaccharides in the pyrolysis volatiles of cellulose which acts as a significant carbon source. Furthermore, structural quality was increased, and organic matrix, defects, and the functional group were decreased, as shown in Figure 10.

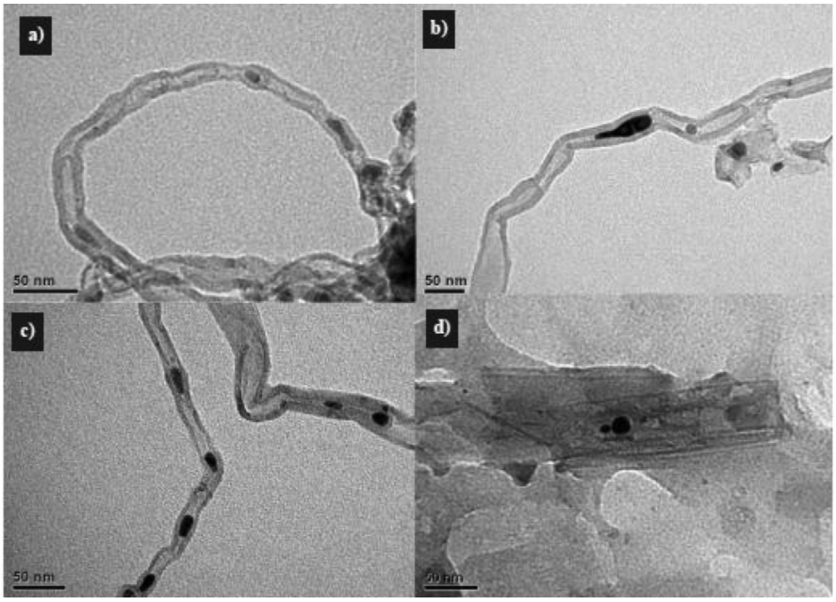

Figure 6. TEM Image of different CNTs derived from biochar produced at 600 °C (a) oat hull, (b) wheat straw, (c) hazelnut hull, (d) rapeseed cake ((a–d) Reprinted from Ref. [12] copyright 2019, with permission from Elsevier).

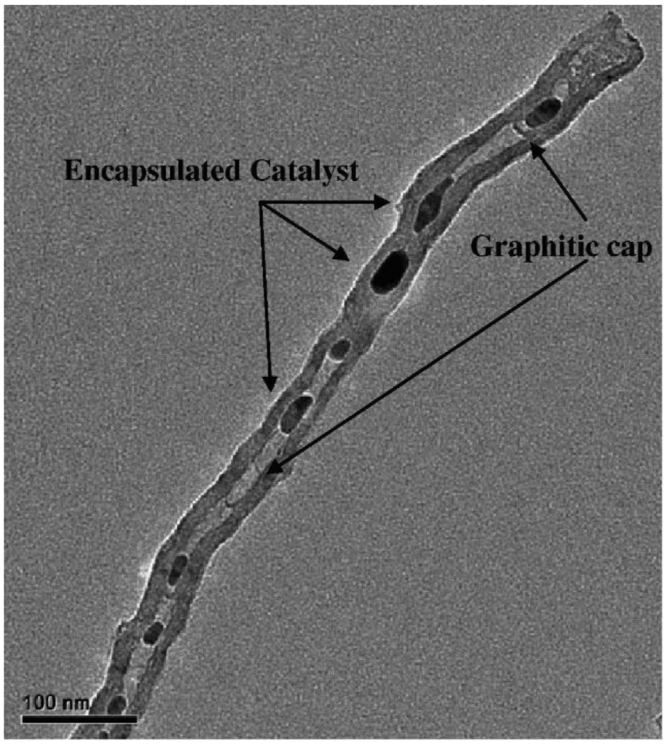

Figure 7. TEM image of Nanoparticle of Fe encapsulated in the CNTs (Reprinted form Ref. [40] copyright 2015, with permission from Elsevier.).

Zheng et al. demonstrated the fast and scalable growth of CNTs at ambient conditions via microwave irradiation, which involves the reaction between 3D MXene aerogel and ferrocene [43]. The MXene aerogel was prepared by mixing sonicated d-Ti3C2 nanosheets and 25 mg of poly (vinyl alcohol), freeze-dried overnight. Figure 11 shows the following steps in the preparation CNTs hybrid.

Ortega-Cervantez et al. developed the MWCNT sponges for the construction of organic transistors (a field-effect OFET device and light-emitting OLET device) in a domestic microwave oven with a maximum yield of 2.2 cm^2 in 12 min [44]. They adopted the mixture of graphite and cobalt acetate powder in an evacuated quartz tube. They reported the diameter of MWCNTs in the 20–50 nm range.

Xie et al. developed a facile microwave method for the fabrication of iron-enriched CNTs on the Poly lactic-co-glycolic acid (PLGA) polymer particles which were coated with Polypyrrole (PPy) [45]. They reported that extensive CNTs were deposited on the surface with a diameter of ~50 nm. Moreover, some hollow CNTs were observed in the HRTEM images, and Fe particles were encapsulated in the tubular structure.

Sridhar et al. reported the facile growth of nitrogen doped CNTs attached over the 3D graphene nanostructure using the microwave synthesis technique [46]. The modified Hummer's method was used to produce graphene oxide from graphite. 3D iron decorated nanostructure of graphene was prepared by the "Doughnut method" using the mixture of iron acetylacetonate, azodicarbonamide (ADC) and graphene oxide in a 0.1:0.3:1 ratio [47]. The mixture was heated by 700 W microwave irradiation for 150 s. The graphene structure was mixed with acetonitrile (ACN) in equal weight ratio and irradiated in a 700 W microwave for 2 min to synthesise nitrogen doped CNTs. The SEM and TEM of produced CNTs are shown in Figure 12 at different magnifications.

Sridhar et al. investigated the microwave synthesis of carbon nanotubes using cobalt and palladium-based zeolitic imidazolate frameworks (ZIF) [48]. Microwave synthesis was carried out in a domestic microwave reactor. The 3D functional nanostructure contained bamboo moulded, nitrogen-doped, micrometre long carbon nanotubes vertically attached to graphene substrate utilizing zeolitic imidazolate frameworks. Results indicate that the 3D nanostructure was mesoporous and had a surface area of 842 m^2/g. Additionally, the prepared nanotube was analyzed in lithium-ion batteries, and high lithium storage capacity of 786 $mAhg^{-1}$ was obtained.

Hazarika et al. produced the silver-loaded multi-layered graphene nanosheet using microwave irradiation (90–100 s) [49]. Fe-loaded carbon nanotubes (Fe-CNTs) were derived from polypyrrole deposited on woven Kevlar fibre using ferrocene by microwave synthesis. It was observed that the tensile strength and impact resistance were improved to 192.56 % and 116.33 %, respectively. Moreover, electrical conductivity was found in the range of $0.75 \times 10^{-2} - 2.2 \times 10^{-2}$ S/cm.

Guo et al. investigate carbon nanotube production using three different feedstock (flake graphite, xGNP, and carbon fibre) and ferrocene using microwave irradiation (10–15 s) and its application on asphalt

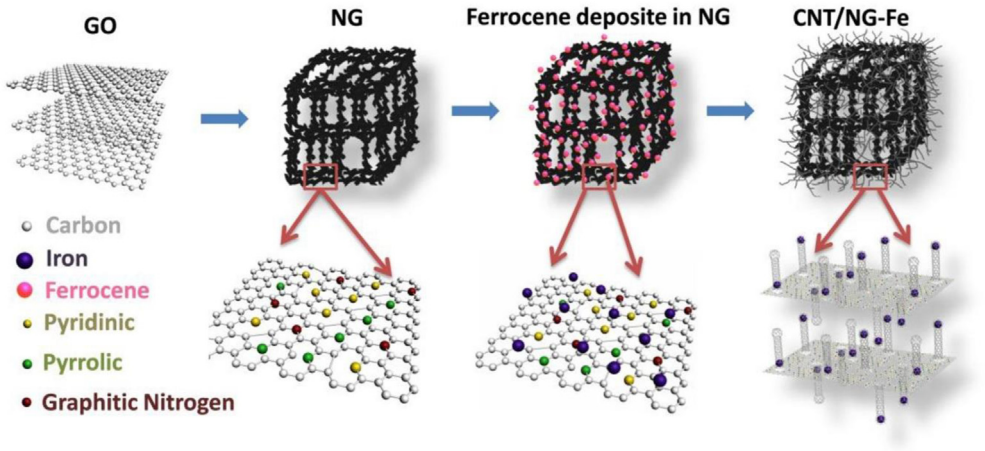

Figure 8. Schematic process of synthesis of CNT/NG-Fe hybrid through microwave irradiation (Reprinted from Ref. [41] copyright 2017, with permission from Elsevier.).

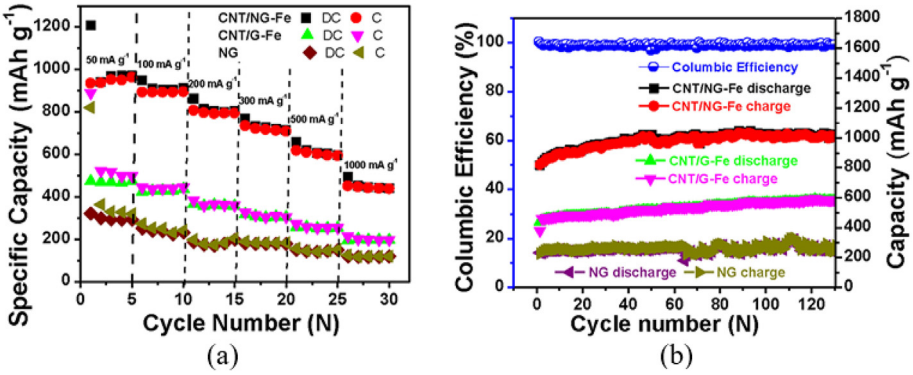

Figure 9. (a) Rate capabilities of the CNT/NG-Fe, CNT/G-Fe, and NG at various rates. (b) Cycle stabilities at 100 mA g^{-1} of the CNT/NG-Fe, CNT/G-Fe, and NG and the columbic efficiency of the CNT/NG-Fe (blue colour). ((a–b) Reprinted from Ref. [41] copyright 2017, with permission from Elsevier.).

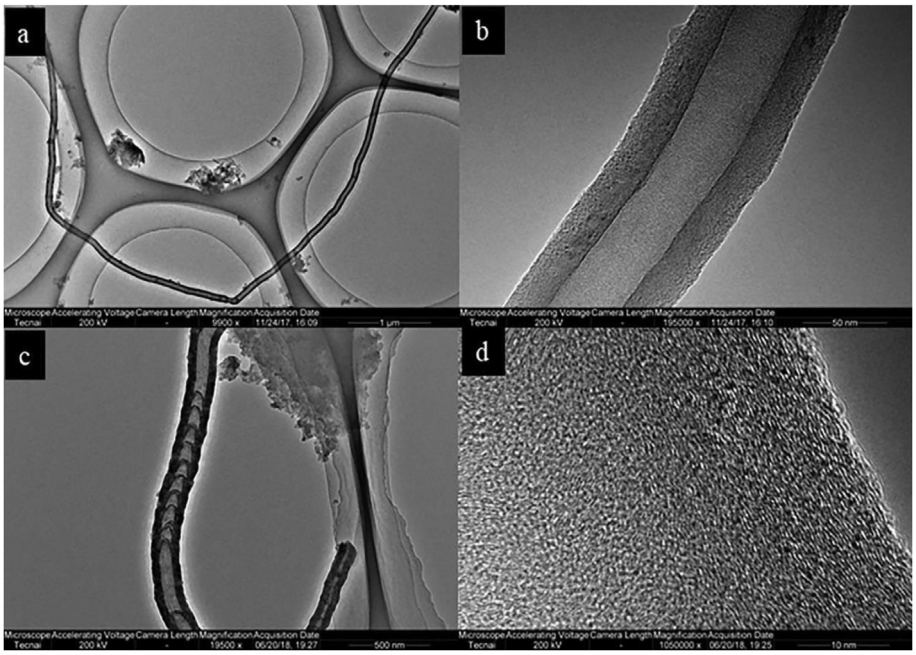

Figure 10. HRTEM images of synthesized CNTs form isolated cellulose at 600 °C through microwave pyrolysis: (a–c) pure and hollow CNTs, (d) Defected CNTs structure (Reprinted from Ref. [42] copyright 2019, with permission from Elsevier.).

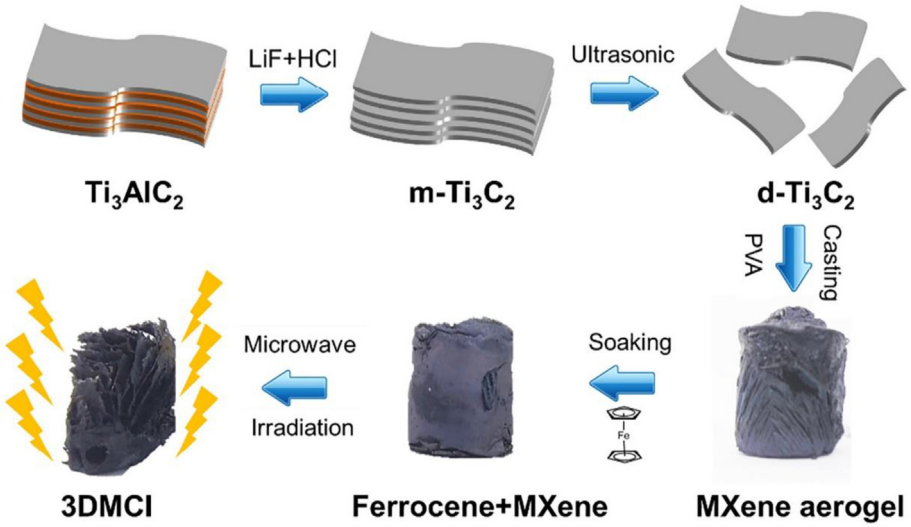

Figure 11. 3DMCI hybrids synthesis process steps (Reprinted from Ref. [43] copyright 2019, with permission from Elsevier.).

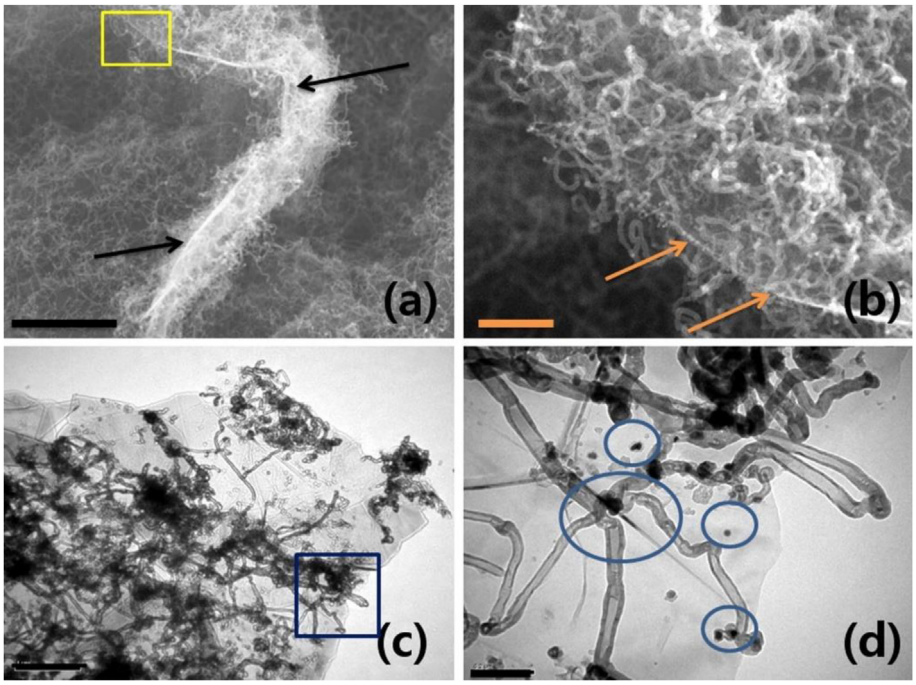

Figure 12. SEM image of nitrogen-doped CNTs over graphene (a) at low magnification with 51 nm scale bar (b) at high magnification with 21 nm scale bar, TEM image of (c) low magnification with 11 nm scale bar and (d) high magnification with a scale bar of 200 nm. ((a–d) Reprinted from Ref. [46] copyright 2015, with permission from Elsevier.).

reinforcement [50]. The results indicated that the dynamic modulus and viscosity were increased in the mixture of asphalt binder and hybrid carbon nanotube. Moreover, at high temperatures, the performance of the modified asphalt binder was enhanced with lowered deformation.

Burakova et al. developed a novel and economical method for carbon nanotube development based on Ni–Mg oxide catalyst using microwave irradiation (0.8 kW and 2.45 GHz) [51]. The effect of microwave radiation on the catalyst surface area was studied. It was observed that with increasing microwave exposure time from 0 to 30 s, the surface area of the catalyst was increased from 5.2 – 9.1 m^2/g. Correspondingly, the catalyst obtained by chemical vapour deposition with modified microwave synthesis for 30 s has increased the yield of carbon nanostructure from (40–45 %).

Benny et al. developed the ruthenium-based single-walled carbon nanotubes (SWCNT-Ru) through microwave irradiation [48]. The synthesis of single-walled nanotubes and ruthenium was carried out in a microwave reactor at 150 °C temperature and 15 min residence time. It was observed that SCWNT-Ru composites derived at 100 °C for 15 min displayed the maximum degradation of Congo red dyes (85 %). In short, SWCNTs play a crucial role in synthesizing non-agglomerate *Ru nano*--elements and cost-effective degradation of the Congo red dye. Different synthesis methods and their condition are shown in Table 2.

Hence, CNTs and hybrids of CNTs were synthesized with the help of microwave irradiation for different applications in a small interval of time. The application part of CNTs is further discussed in the application section. The mechanism of the CNTs growth from microwave heating

required more deep research to unlock the potential of the microwave irradiation synthesis technique.

3.5. Other synthesis techniques

Apart from the above techniques, CNTs were synthesized using modifying existing techniques and novel techniques. The CVD method has been modified throughout the years by utilizing its different forms such as vapor phase growth CVD, plasma-enhanced CVD (PECVD), thermal CVD (TCVD), photothermal CVD (PTCVD), floating catalyst CVD (FCCVD), aerosol-assisted (AACVD) or liquid pyrolysis, aerogel-supported CVD, laser-assisted CVD, remote plasma CVD, microwave-assisted CVD and alcohol catalytic CVD [52]. Similarly, arc-discharge and laser ablation techniques were modified by changing the operating condition and materials (i.e., catalyst, power, temperature, pressure and working environment). Further researchers developed new methods for the development of CNTs efficiently for example, flame synthesis method, solid-state pyrolysis [53], bottom-up organic approach [54], ball

Table 2. Different methods and their conditions to synthesized CNTs.

Synthesis Methods	Catalyst and substrate	Carbon source	Temp. (°C)	Time	Flow rate of gases (ml/min)	Product Quality	References
CVD	Co/Al substrate	CH_4	2100	15 min		VACNT (d:9 um)	[60]
	Ni/Co–TiB_2	C_2H_2	900		C_2H_2~100 ml/min	CNT-Co@TiB_2	[61]
	NiO/HZSM-5 zeolite	PP	500–800	35 min	Plastic feed rate 80 g/h, Hydrogen gas concentration 72.21 vol.%	MWCNTs (15–25 nm)	[62]
	Co–TiO_2	Hexane	700–800	10–30 min	Hexane ~150 ml/min	MWCNTs (d: 15–30 nm)	[63]
	Cu/$CaCO_3$	Pyrolysis gas	800	3 h	Pyrolysis gas	MWCNT	[64]
Arc- discharge	Ni/Y	Graphite rod			30V & 95A Ar ~1.43 cm^3/min; 39kPa	MWCNT (d:24 nm and L: 690–1680 nm)	[65]
	Fe	Graphite rod			12kPa; 90A	Fe2O3/CNT (d:10 nm)	[66]
	Mixture of Carbon, paraffin & ZnO powder	Graphite rod		20 s	500 Torr, 80A	ZnO-CNT (3–10 nm)	[67]
	Si/Ni	Ethanol		30 s	4.5A	Ni-filled/CNT (d:10 nm & L: 20–150 nm)	[68]
	Fe/FeS	Graphite rod		20 min	50 Torr, 80A	DWCNT (2–7 nm)	[69]
Laser ablation	Co–Ni	Graphite rod	1200	12 h	500 Torr Ar~50 sccm Continuum laser DCR-16S/	SWCNT (d:1–2 nm)	[32]
	-	Graphite powder mixed Ni, Co, FeS	1150		0.5bar Ar, H2~ 80 sccm, ND:YAG laser	SWCNT (d:20 nm)	[35]
	-	Graphite Ni/Y composite	1100		50–500 torr Ar & He, CO2 continuous wave	SWCNT (d: 10–20 nm)	[70]
	C, Co, Ni	Graphite powder mixed with Ni/Co	1100–1350		Ar, XeCl excimer laser	SWCNT (d:1.2–1.7 nm, L:>2 um)	[71]
	-	Composite of C/Co, C/Co/Ni	Room temperature		2 Torr Ar & O_2, KrF excimer laser	SWCNT (d:100–200 nm, L:1–2.5 um)	[71]
Microwave Irradiation	Fe, activated carbon fibre	Activated carbon fibre	-	30–120 s	Ar~1.67 × 10^{-6} m^3/s	MWCNT (13 nm)	[72]
	Ferrocene	Ferrocene	-	20–40 a	-	CNTs (10–160 nm)	[37]
	Co, Graphene oxide	Zeolitic imidazolate frameworks		30 s		Graphene/Co/N-doped CNT hybrids	[48]
	Ferrocene, Kevlar fiber	Ferrocene	1100	90–100 s		Fe-CNT/Ppy-coated Kevlar fiber	[49]
	Ferrocene, Ti_3C_2 (MXene)	Ferrocene		20 s		3D metal oxide/ carbon nanotube/ iron hybrids	[43]
	Fe, Graphene Ferrocene,	Azobis		2 min		Graphene-CN Hybrids	[46]
	Ferrocene, Acetylacetonate	Ferrocene, azodicarbonamide		190 s		3D CNT/N-doped rGO/ Fe hybrids	[41]
	Cobalt acetate, Graphite	Cobalt acetate		3–12 min		MWNT sponges	[44]
	Palladium acetate, Graphite oxide	Palladium acetate		3 min		Pd-CNT-rGO Composite	[38]
	Ferrocene, Exfoliated graphite Nanoplatelet (xGNP)	Ferrocene		10 s		MWNT coated Graphite	[50]
	Ferrocene, Graphite	Ferrocene		30 s		MWCNT (45–79 nm)	[39]
	Ferrocene.	Ferrocene		15–20 s		MWCNT (20 nm)	[73]
	Ferrocene, Fly ash	Ferrocene		15–30 s		MWCNT coated fly ash	[62]
	Ferrocene, Graphite	Ferrocene		5 s		MWCNT (24–45 nm)	[40]
	Ferrocene, Ti_3C_2	Ferrocene		40 s		CNT@Ti_3C_2 hybrids	[74]
	Ferrocene, Reduced graphene oxide (rGO)	Ferrocene, azodicarbonamide		180 s		3D rGO/CNT/Fe	[75]
	Ferrocene, Poly (lactic coglycolic acid) (PLGA)	Ferrocene		10–20 s		CNT-Fe-PLGA Particles	[45]

milling [55], direct and wet spinning (CNTs fibres) [56], hydrothermal [57] and electrolysis method [58].

4. Characterization of CNTs

4.1. Dynamic light scattering (DLS)

This technique provides information related to the hydrodynamic diameter CNTs. The dispersion of CNTs in liquid solution is determined by DLS [76]. In other words, the particle size distribution of CNTs is determined by DLS measurement. The Stoke-Einstein equation is used to determine the hydrodynamic diameter and length distribution of CNTs agglomerates in liquid solution [77, 78, 79].

Reinert et al. reported the hydrodynamics radius for the number fraction of particles in the ultrasonic bath for different treatment times, as shown in Figure 13. It was observed that ultrasonic treatment decreased the radius of particles from 250 nm to 40–70 nm in the first 20 min, and further treatment does not affect the hydrodynamic radius [76]. Hildago-Oporto et al. observed the hydrodynamics diameter of 140 nm, 400 nm, 180 nm, and 300 nm at 400 °C pyrolyzed biochar CNTs and 130 nm, 70 nm, 70 nm, 150 nm at 600 °C pyrolyzed biochar CNTs of oat hull, wheat straw, hazelnut hull and rapeseed cake, respectively.

4.2. UV- visible absorption spectroscopy

UV- visible Absorption spectroscopy is used to identify the concentration and optical properties of CNTs. Beer-Lambert's law is used to determine the concentration of CNTs in solution. According to this law, the concentration of solute in a solution is directly proportional to the absorbance and surging in intensity peaks with an increment in CNTs concentration [80]. Hildago-Oporto et al. reported the surge in peak intensity for all CNTs produced from pyrolyzed biochar at 400 °C and 600 °C, as shown in Figure 14. Previous studies observed the maximum peak of absorbance for the CNTs sample in the range of 230–250 nm [12, 39, 77, 81, 82]. For different biochar derived CNTs, the UV absorption spectra are shown in Figure 14(a-d).

Due to the plasmon resonance of free π electrons of CNTs unique band is observed at 240 nm wavelength in the UV region [83]. UV–vis absorption spectra help to determine the optical energy band gaps of CNTs.

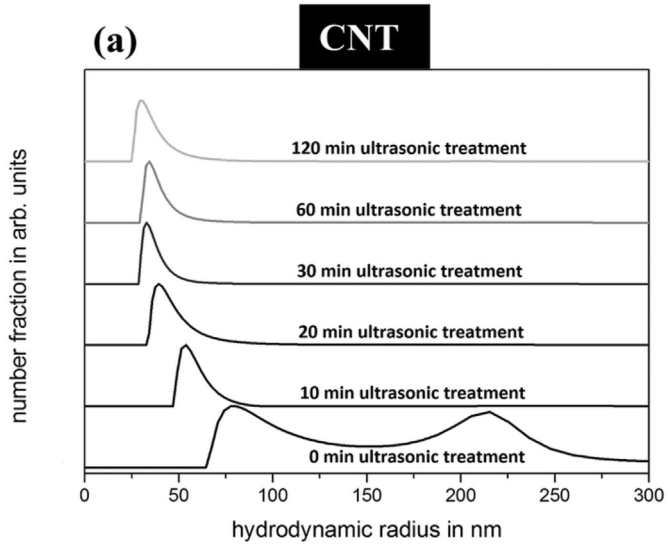

Figure 13. DLS data of (a) CNT in ethylene glycol after different times of ultrasonic treatment (Reproduced from Ref. [76] with permission from the Royal Society of Chemistry).

According to Johan and Moh, the optical energy band gap is calculated with the derivative Tauc plot with the help of the following equation:

$$\propto(h\nu) = A\left(h\nu - E_g\right)^n \quad (1)$$

Where as,

h = plank constant
ν = frequency of incident light,
$\propto$ = absorption coefficient,
E_g = optical energy band gap of the material
A = the probability parameter for the transition,
n = nature of the transition, which has a value equal to 1/2 for an allowed direct transition [84].

The plot of the energy band gap with photon energy for biochar derived CNTs at 400 °C and 600 °C is shown in Figure 15. Hildago-Oporto et al. showed a decrease in hydrodynamics diameter with an increase in energy band gap with corresponding CNTs, as shown in Figure 17 [12]. According to Collins et al. specific CNTs, the energy band gap is inversely proportional to its diameter [85]. Khalizadeh reported the smaller particle size with a high energy band gap shows the quantum confinement phenomenon [84]. On the opposite side, the energy band gap decreases as the hybridization of σ and π orbitals occurs [83].

4.3. Raman spectroscopy

The degree of wall graphitization and identification of SWCNTs or MWCNTs is determined by Raman spectroscopy. It is a very robust and quick technique to identify carbon samples. RBM (Radial breathing mode) peak is one of the essential features of Raman Spectra, which is observed between the wavelength of 100–250 cm^{-1} [86, 87]. The appearance of the RBM peaks confirms the presence of the SWCNTs or MWCNTs. The appearance of RBM peaks confirms the presence of SWCNTs, and on the other side, the low intensity of RBM peaks confirms the presence of MWCNTs, as shown in Figure 16 (a). The RBM peak is absent in the pure graphitic structure. According to Dresselhaus and Eklund, more interaction between the carbon layers in MWCNTs causes lower intensity and broadens the RBM peak. The diameter of nanotubes (d_t) is inversely proportional to the frequency of the RBM peak with relation as [86, 87, 88]:

$$d_t = \frac{248}{\omega_{RBM}\ (cm^{-1})} \quad (2)$$

Where as,

ω_{RBM} = frequency of RBM peak (cm^{-1})
d_t = diameter of CNT (nm)

Two significant peaks appeared at a frequency between 1300 and 1590 cm^{-1}. The first peak was observed at 1330-1360 cm^{-1} called D mode or D-band. The D-band symbolises sp^3 hybridization of carbon atoms, the defects or disordered carbon atoms in CNTs. It is caused by vacancies, pentagon or heteroatoms, high-density defects and breathing modes present in CNTs [40, 89, 90, 91]. The second peak appears near 1580 cm^{-1} called G-band or G-mode. It represents the ordered carbon structure of CNTs. G-band signifies the sp^2 hybridization of carbon atoms and graphitic structure of CNTs [40, 90]. The G-band of MWCNTs, SWCNTs and graphite is illustrated in Figure 16(b). The third peak is also observed near 2686 cm^{-1} or in the range of 2500–2900 cm^{-1}, which is a dominant feature of the second-order Raman spectrum called the 2D-band [36]. 2D-band is also called overtone mode of G band, which indicates the double phonon resonance. The second-order 2D-band is detected even in crystalline graphite, where the disorder-induced D-band is absent, implying that the 2D-band is an inherent characteristic of the

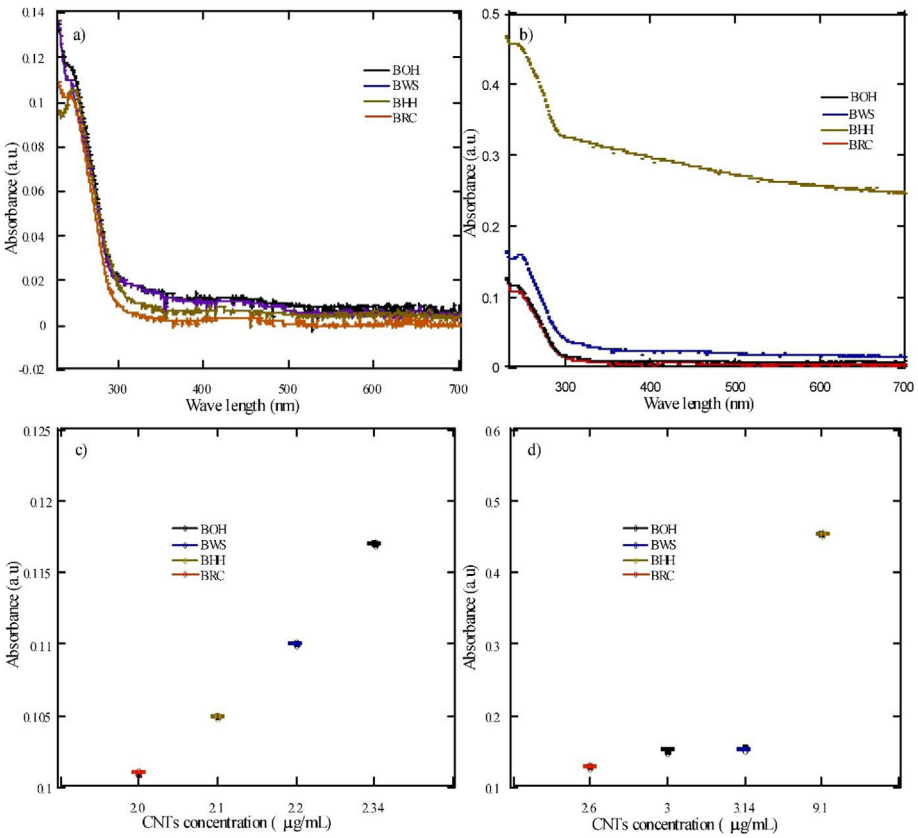

Figure 14. UV–vis absorbance spectra of CNTs suspensions in aqueous sodium dodecyl sulfate (SDS) synthesized from a) Biochar pyrolyzed at 400 °C b) Biochar pyrolyzed at 600 °C. Concentration plot for the absorption peaks of CNTs synthesized from c) Biochar pyrolyzed at 400 °C d) Biochar pyrolyzed at 600 °C ((a–d) Reprinted from Ref. [12] copyright 2019, with permission from Elsevier.).

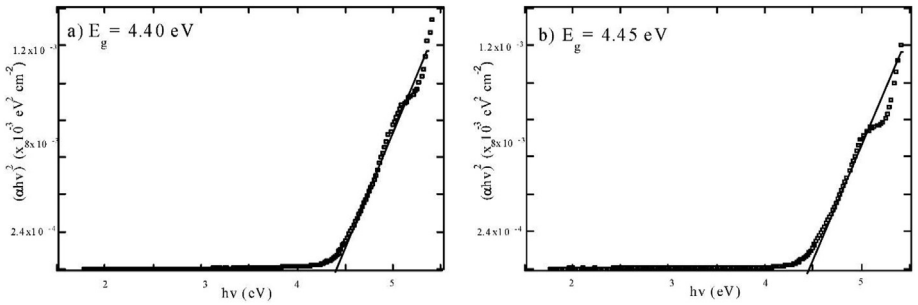

Figure 15. $(ahv)^2$ versus hv (eV, photon energy) plots of CNTs synthesized from a) BOH pyrolyzed at 400 °C b) BOH pyrolyzed at 600 °C ((a–b) Reprinted from Ref. [12] copyright 2019, with permission from Elsevier.).

2D graphene lattice. The more graphitic structure of CNTs is shown by the presence of the 2D-band. The quality and crystallinity of CNTs are determined by the intensity ratio (I_D/I_G) of the D-band to the G-band [92]. Better quality and a high degree of wall graphitization are observed when I_D/I_G ratio is low [39, 93]. Han et al. reported the I_D/I_G ratios 0.47, 0.48, 0.59 and 0.49 for SF-made, Mo-made, Fe-made and Cu-made CNT, respectively as shown in Figure 16(c) [37]. Guo et al. found the I_D/I_G ratio between 0.854 and 1.04 for CNTs with and without hydrogen protection [50].

4.4. Thermogravimetric analysis

This analytical technique is used to check the thermal stability of the CNTs and monitor the fraction of components such as moisture, volatile matter, graphitic carbon and ash formation on the basis of weight loss at a specific temperature of the CNTs [95]. The procedure is performed in the presence of Oxygen or inert gases like nitrogen, argon and helium. The weight loss is recorded as a function of temperature. Slow oxidation is performed to analyze material properly [96].

Zhan et al. reported that less than 10 % weight loss occurs around 400 °C, indicating the degradation of amorphous carbon. Moreover, 70 % weight loss was observed between 500-600 °C, which indicates an intense peak of differential thermogravimetry curve (DTG) in Figure 18 (d). This maximum weight loss corresponds to combustion of CNTs. The temperature above 600 °C, the weight loss shows the residual iron metal catalyst degradation. The peaks around 200 °C show the combustion of the ferrocene catalyst used for synthesis [37]. Asnawi et al. observed the 10 % loss of amorphous carbon taking place at 343 °C and 90 to 4.6 % material decomposes around 343–490 °C. and significant peaks of DTG curve obtained at 421.5 °C, which shows the 50% weight loss of synthesized CNTs as shown in Figure 17 [36].

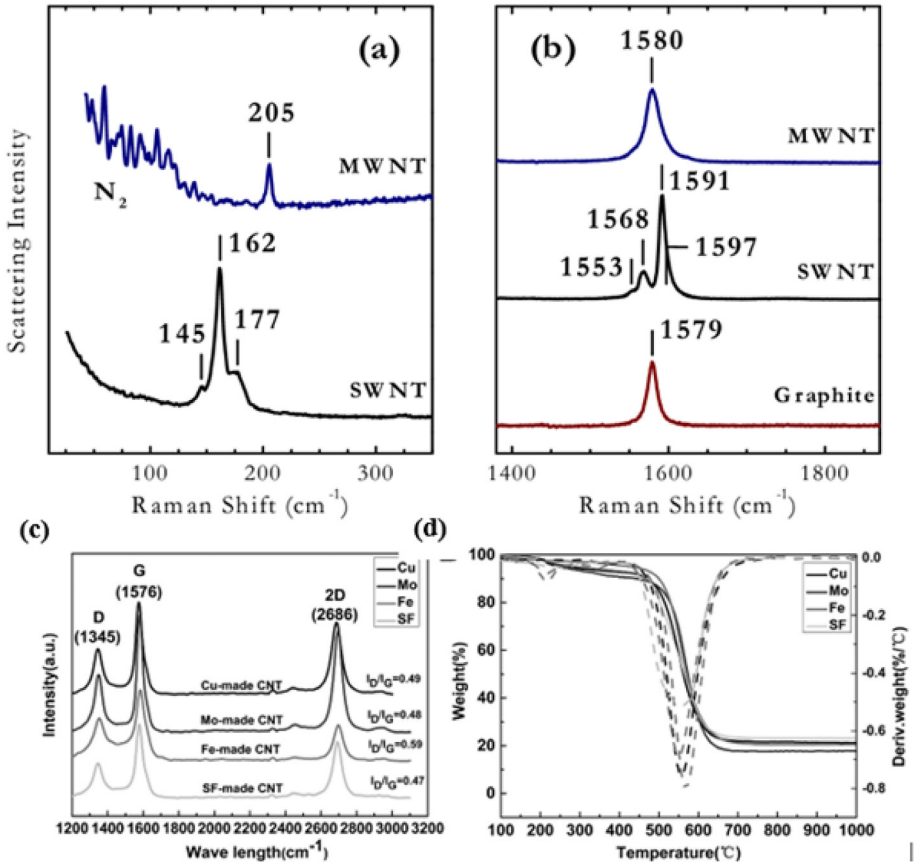

Figure 16. (a) Low and high energy intensity regions of SWCNTs and MWCNTs in RBM. (b) Comparison of the Raman spectra of SWCNTs, MWCNTs and graphite [94c] Raman spectra of metal material derived CNTs (d) Thermogravimetric analysis of metal material derived CNTs (Reprinted from Ref [37] copyright 2017, with permission from Elsevier.).

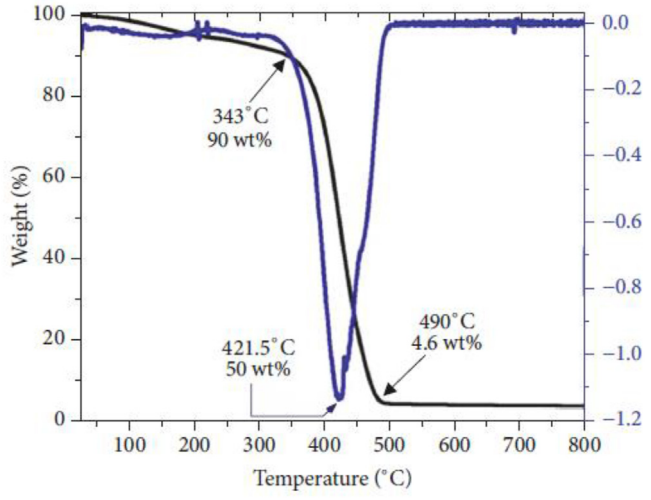

Figure 17. TGA and DTG graph of synthesized CNT [36].

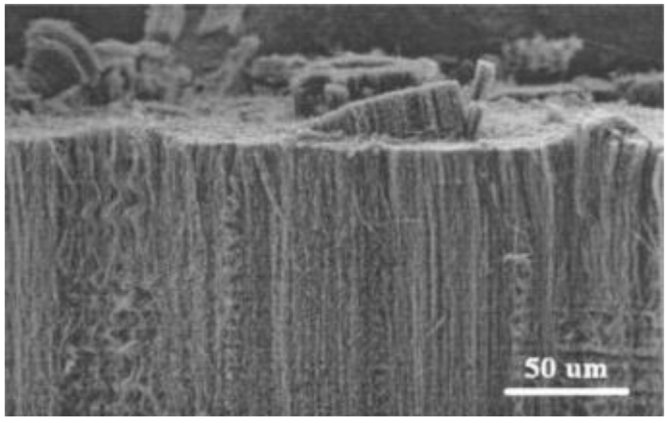

Figure 18. (SEM) image of Aligned CNTs (Reprinted from Ref. [97] copyright 2019, with permission from Elsevier.).

4.5. Scanning electron microscopy (SEM)

The topography, crystallographic, surface morphology of CNTs was studied using this technique [95]. The structure information of CNTs, such as diameter and length, is examined by SEM. In this, a beam of electron passes over the surface of the materials or scanning, where a charge is accumulated, and image formation takes place, as shown in Figure 18 and Figure 19 (a) [97]– [99].

4.6. Transmission electron microscopy (TEM)

This tool is used for finding the metal impurities in structure, exact diameter and length measurements. It is different from SEM because in TEM, a beam of an electron is transmitted through the surface of material or sample and image formation takes place at the phosphor screen [100, 101]. SWCNTs and MWCNTs are differentiated by observing the high-resolution TEM image as shown in Figure 20 (a-b and d). Figure 19 (b) and Figure 20 (c) shows an example of TEM image [35, 97]

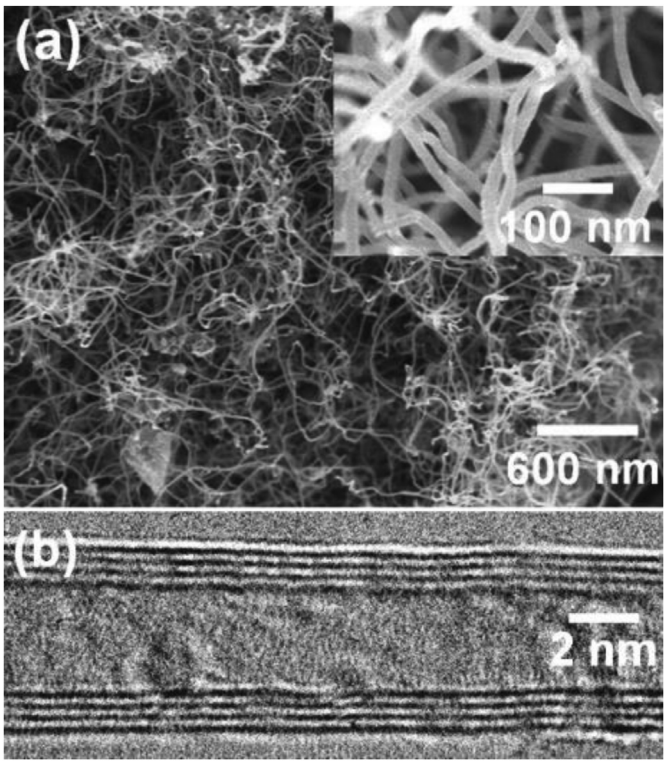

Figure 19. (a) SEM image of synthesized CNT on flexible Co/Cr/Teflon substrate and (b) TEM image of the synthesized CNTs on flexible Co/Cr/Teflon substrate through microwave irradiation. (Reprinted with permission from [98]. Copyright (2005) American Chemical Society.).

4.7. X-ray diffraction (XRD)

XRD tells about the molecular and atomic structure of a crystalline substance. It is an analytical technique in which X-rays interact with the crystalline phase, and the beam is diffracted in many directions. On measuring the angles of these diffracted beams, the electron density of the crystal is measured. This electron density gives the idea about the chemical bonds, mean position of an atom in the crystal and disorder in phase provide information about the unit cell dimensions. In CNTs, a graphitic peak is observed around 26.1° [104]. Zhan et al. observed the CNTs peak C (002) at 26° and iron catalyst crystal (Fe) peak around 45° and 65° in the XRD pattern. The oxidation of iron particles in the air atmosphere was taking place, which formed Fe_2O_3, and their peaks were observed around 30°, 35° and 50° as shown in Figure 21 [37].

4.8. X-ray photoelectron spectroscopy (XPS)

This is a surface-sensitive quantitative spectroscopic technique used to assess the elemental composition of the surface of the sample. The chemical composition of the outermost layers of the CNTs was characterized by X-ray photoelectron spectroscopy (XPS). Kang et al. reported that using wide XPS spectra, CNT/NG-Fe found C, N, O and Fe at 285.0 eV, 533.0 eV, 399.0 eV and 711 eV, respectively, as shown in Figure 22(a) [41]. Four deconvoluted peaks were visible in the binding energy region plot of C 1s, with their centres corresponding to the C=C, C–N, C=N, and C=O bonding at 284.8 eV, 285.8 eV, 286.9 eV, and 289.1 eV, respectively in Figure 22(b). Two significant peaks in the high-resolution N 1s spectra, centring around 398.2 eV and 401.3 eV, respectively, were identified as pyridinic and graphitic-N, respectively, as shown in Figure 22(c). These peaks indicated the incorporation of two major N configurations. Additionally, two minor peaks corresponding to pyrollic and oxidised pyridinic-N bonds were seen at about 399.1 eV and 404.5 eV.

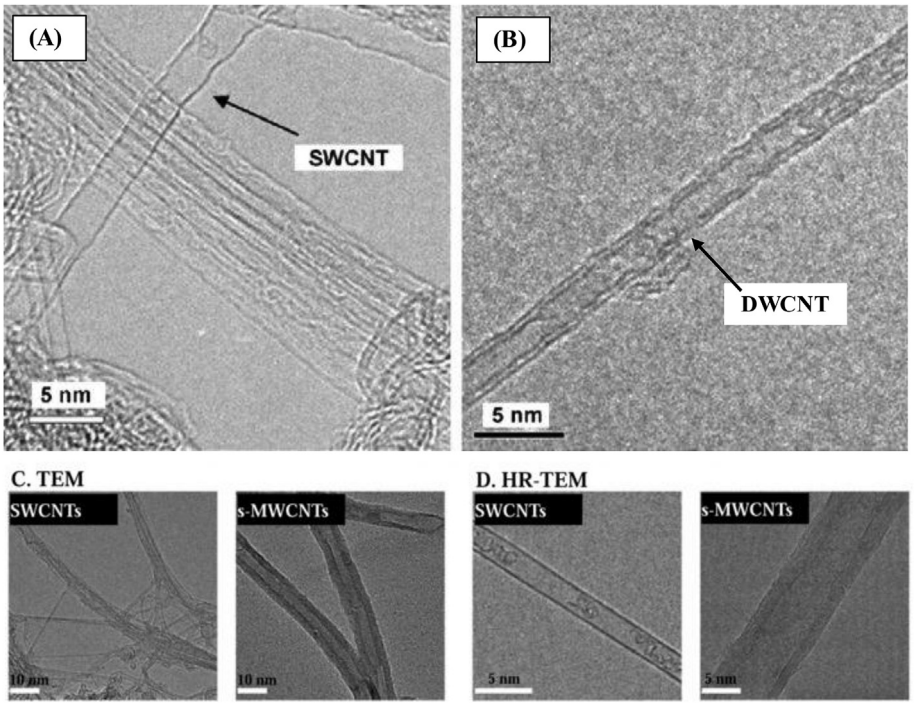

Figure 20. High resolution TEM image of (A) SWCNTs (B) DWCNTs (Reproduced with from Ref. [102] copyright 2012, with permission from WILEY-VCH Verlag GmbH & Co. KGaA, Weinheim.) (C) TEM image of SWCNTs and MWCNTs (D) HRTEM image of SWCNTs and MWCNTs (Reproduced with from Ref. [103] copyright 2013 with permission from WILEY-VCH Verlag GmbH & Co. KGaA, Weinheim.).

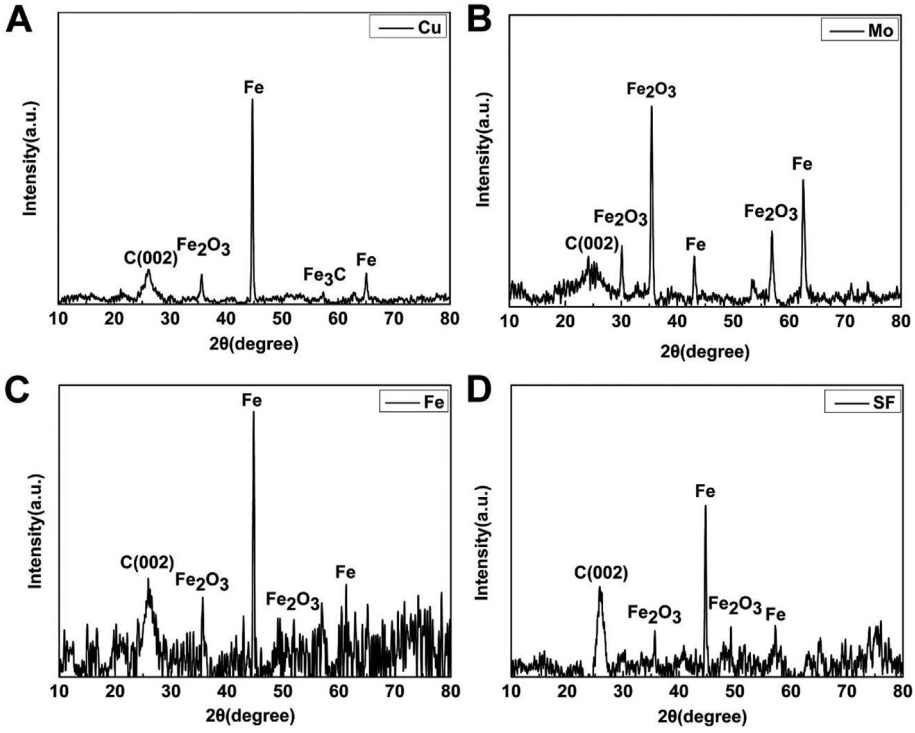

Figure 21. XRD image of (A) Cu-wire CNT, (B) Mo-wire CNT, (C) Fe-wire CNT, (D) steel fibre CNT ((A–D) Reprinted from Ref. [37] copyright 2017, with permission from Elsevier.).

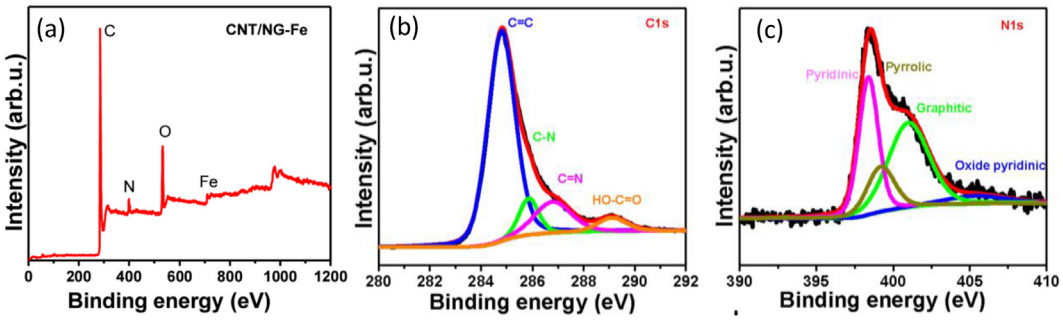

Figure 22. (a) Full scan of the CNT/Ng-Fe, High resolution scan (b) C 1s and (c) N1s (Reprinted from Ref. [41] copyright 2017, with permission from Elsevier.).

Zheng et al. demonstrated the XPS spectra of pristine Ti_3C_2 and CNT@Ti_3C_2 in Figure 23(a) [74]. In the XPS scan of Ti_3C_2 the elements like Ti, C, F and O were detected, while in CNT@Ti_3C_2, the Fe element was also noticed. The Fe element is an indication of the growth of CNTs through microwave irradiation using a ferrocene catalyst. In Figure 23(b), the high-resolution XPS C 1s spectrum of pristine Ti_3C_2 includes bonds such as O–C=O (288.85 eV), C–O (286.50 eV), C–C (284.58 eV), and C–Ti (281.51 eV). There are only C–O (286.10 eV) and C–C (284.83 eV) bonds in CNTs@Ti3C2-III (Figure 23(c)). The peak intensity of C–C appears to be increased, indicating an abundance of CNTs on the surface of Ti_3C_2. Furthermore, the disappearance of C–Ti peaks can be attributed to CNT coverage on the MXene and external Ti_3C_2 transformation to other phases.

There are other techniques also used to find out the mechanical and electronic properties of the CNTs. But here in this literature, general characteristics of the CNTs like their size, quality, structure, optical properties, crystallinity, surface composition and thermal properties techniques were reviewed. Due to the small sample size and the nanometre size, characterization of the CNTs becomes a very tedious and time-consuming process. Further research must be needed to simplify the characterization process. In addition, new image processing software and quantitative models should be developed to easily find out the properties of CNTs.

5. Applications of CNTs

Due to excellent chemical and physical properties such as high thermal stability, ultralight weight, high thermal conductivity, high electrical conductivity, and high mechanical properties (tensile strength), CNTs applications have gained much attention among researchers.

5.1. Metal oxide nanocomposites

Since the last decade of the century, to prepare a hybrid structure of carbon, various type of combination of metal oxide with carbon nanotube was experimented. Metal oxide of titanium, tin, aluminium, zinc, zirconium, iron etc., were mixed with pristine carbon nanotubes. The synthesized nanohybrids are used in the development of nano devices which have numerous applications in photodetectors, lithium-ion batteries, photoelectrode, photocatalytic, sensors, supercapacitors, and absorbents.

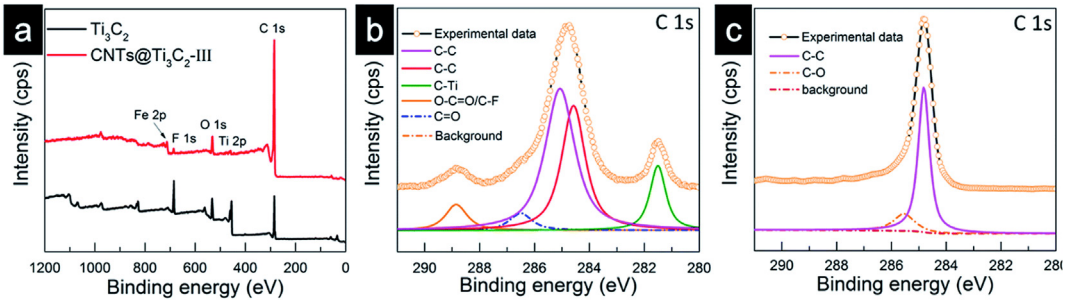

Figure 23. (a) Full scan of Ti_3C_2 and CNT@Ti_3C_2 (b) C1s of Ti_3C_2 (c) C1s of CNT@Ti_3C_2 (Reproduced from Ref. [74] with permission from the Royal Society of Chemistry.).

The physical properties such as electrical conductivity, electron mobility, thermal conductivity, resistivity, elastic modulus specific gravity, thermal stability in air and coefficient of thermal expansion of SWCNTs and MWCNTs helped in making nanohybrids [105, 106]. The increase in hardness (9.98 GPa) and high toughness (4.7 MPa $m^{1/2}$) was achieved by CNT/Al_2O_3 nano composites using the CVD synthesis method [107]. According to Yamamoto et al., synthesized nanocomposites of alumina to attain high-temperature stability and high toughness [108]. The alumina nanocomposite fracture toughness and bending strength were found at 5.09 MPa $m^{1/2}$ and 689.6 ± 29.1 MPa, respectively. Hybrid adsorbent CNT/Al_2O_3 was prepared using the sol-gel method, and impurities like diclofenac sodium and carbamazepine were removed with sorption capacities of 157.4 and 106.5 μmol/g, respectively [109].

Keshri et al. incorporated the homogenous mixture of 1.5 wt.% of CNT mixed with alumina coated on the steel substrate and achieved a 25 % increment in fracture strength and toughness [110]. The Reactive Red 198 and Blue 19 dyes were removed using CNT/Al_2O_3 hybrid nano composite from the wastewater, and removal efficiency of 91.54 % and 93.51 % were accomplished [111]. Traces of ammonia gas were sensed using the CNT/Al_2O_3 hybrid film-based sensors. A fast response time of 10 min and detection of NH_3 gas up to 6 ppm were acquired [112]. Liu et al. showed the photocatalytic efficiency of the ZnO/MWCNT hybrid composite was three times higher than the pure nanowire of ZnO [113]. Kaur et al. synthesized graphene oxide based CNTs field emitter on nickel and demonstrated a high enhancement factor (15,999), emission current density of 64 mA/cm^2 and lower turn-on field of 0.71 [114]. A nanoscale hybrid of n-WO_3 and MWCNTs was fabricated to sense nitrogen dioxide. The composite with 0.5% MWCNTs sensed the 5-ppm nitrogen dioxide in ~80 s/~300 s at 150 °C [115]. Yan et al. used the solvothermal method to synthesize reduced MOF-818@graphene oxide (rGO)/MWCNTs composite [116]. The prepared hybrid has high electrical conductivity and active sites with a hierarchical porous structure. MOF-8182 rGO/MWCNT hybrid has good electrochemical sensitivity for phenolic acids in biological samples such as chlorogenic acid, gallic acid and caffeic acid [43]. CNT/MO hybrids have the potential to become next-generation functional materials for a wide range of applications with significant societal impacts, such as photocatalysis, lithium-ion battery, supercapacitors, photovoltaics, and sensors. As the quest for a "greener" or "environmentally friendly" future continues, the commercial adoption of hybrids with high efficiency and low cost will grow.

5.2. Energy conversion and storage devices

In manufacturing renewable energy conversion and storage devices, SWCNTs and MWCNTs are gaining plenteous attention at the world level. Exceptional optical properties like high thermal conductivity and electron mobility in CNTs make them convenient for energy conversion and storage devices [117]. Application in making different devices as follows:

In the 21st century, transparent conducting films (TCFs) are widely used in liquid crystal displays, touch screens, organic light-emitting displays and PV cells. Due to the rapid demand for TCFs in the global market, various techniques have been developed to fabricate cost-effective and eco-friendly TCFs. However, conventional materials such as a metal oxide of Indium and fluorine are used to fabricate TCFs which have less flexibility [118]. Recently, to add more flexibility to TCFs, SWCNTs and MWCNTs has been used. CNTs based TCFs have 1–100 nm thickness, resulting in excellent optoelectronic properties such as electrical conductivity, optical transmittance, and sheet resistance [119, 120, 121]. In PV cells, CNTs based TCFs show superior work function, low sheet resistance, good surface roughness and high stability [122, 123]. Different dry and wet process approaches such as spin coating, spraying, CVD, filtration transfer, Langmuir Blodgett deposition, and laser ablation have been used to synthesize CNTs based TCFs [123, 124, 125, 126, 127]. The dry synthesis process developed fewer defects and a more refined quality of CNTs based films. According to Kaskela et al., in dry processed CNT based films, low resistance of 110 Ω/cm^2 with 90 % transmittance has been observed [128]. In contrast, the industry favours the low-cost wet process CNTs films because of less operating temperature. Despite the low-cost efficiency of present TCFs, it is highlighted that CNT-based TCFs have tremendous promise for usage in stretchy, flexible, and wearable electronics.

5.3. Biomedical sector

In the field of biomedical science, CNTs have a wide range of applications in biomolecule drug delivery to targeted organs, biosensors diagnosis and analysis. The surface of CNTs is functionalized to increase their solubility, which is further derivatized with active molecules to make them compatible for biological system applications. CNTs are classified into two types depending on the presence of carbon layers, namely SWCNTs consisting of single graphene layers with diameters between 0.4 and 2 nm and MWCNTs made of 1–3 nm diameters graphene sheets comprising two or more cylinders.

The major concerning factor in biomedical application is the level of purity. Hence, the carbon nanotubes need to undergo macroscopic processing to improve quality and other desirable characteristics in length, alignment etc, depending on the application.

5.3.1. Application in biosensors

MWCNTs have significant potential in biosensors application for supporting immobilization of protein while maintaining the inherent activity of protein which makes them attractive for application in biosensors.

5.3.1.1. Electrochemical biosensor. CNT biosensors with definite elements of bio receptors are combined with an electrode that changes the computable electrical signal to identify targeted compounds in the sample. Due to the speed, portability, specificity, and low cost of biosensors, they find clinical application in decentralized testing sites. Revathi et al. used amine functionalized MWCNTs to create an electrochemical sensor for the nonenzymatic detection of hydrogen peroxide

[129]. For the simultaneous detection of two nitrogenous bases, namely guanine and adenine, Wang et al. developed a nano sensor based on MWCNTs and Copper-nickel hybrid nanoparticles [130].

5.3.1.2. Piezoelectric sensor. The design of the piezoelectric sensor based on MWCNT was done by exploiting the electromechanical properties. The CNTs were made uniform and compact, which played a significant role in the sensor fabrication. In order to measure pressure without the aid of deformation materials, Ramalingame et al. constructed a stretchy sensor using MWCNTs on a PDMS substrate [131]. Ali et al. created a piezoresistive sensor out of graphene, CNTs, and graphene-CNTs composites [132].

5.3.1.3. Gas sensor. Nano scale sensing interface proves advantageous in terms of selectivity and sensitivity of gas sensors. These sensors provide an alternative solution to the conventional gas sensors, which are otherwise bulky and require skilled labour. Changhoon Song et al. designed a NO_2 gas sensor by patterning the MWCNTs onto NOA 63 polymer and were energized by an integrated supercapacitor. The designed sensor was able to attach to the skin defects [133].

5.3.2. Drug targeting:

Target drugs are useful in delivering treatment to precise parts that require drug delivery for an extended period. MWCNTs have applications in targeting drugs for treatment and releasing drugs in a controlled manner through magnetic stimulus, electric stimulus, temperature change, and others. Due to the hydrophobic nature of CNTs, drug delivery in the human circulation system stays for an extended period and acts as carriers for the transportation of biomolecules like protein, DNA and RNA, immunoreactive compounds and lectins. Seyfoori et al. discussed the involvement of MWCNTs and pH-responsive gels in the delivery of the medication duxorubicin. The developed nanohybrid system was designed to deliver the drug to U-87 Glioblastoma cells, and it was discovered that tumour proliferation was limited when the treatment was supplied via a nanohybrid system [134].

5.3.3. Treatment and diagnosis of cancer:

Wang et al. established that narrow multi-walled nanotubes. Narrow MWCNTs application in cancer treatment resulted in the improved affinity of tissues resulting in high tissue accumulation [135]. Hence a higher aspect ratio of narrow MWCNT proved beneficial for the biological application. Samori et al. used multi-walled carbon nanotubes to administer the anticancer medication methotrexate in vitro via an enzymatic cleavage release mechanism in breast cells [136].

5.3.4. Application as antibacteria

The aspect ratio of MWCNTs influences the antibacterial property to a large extent. The short tube was reported to allow more interaction with the cell membrane than the long tube MWCNTs [137]. Depending on the aspect ratio of MWCNTs, the anti-bacterial property can be determined. Small diameter led to close microbes' interaction while large-sized ones led to lesser interaction with microbes [138].

5.3.5. Application as antifungus

The CNTs composites showed great potential in the inhibition of spore germination. Studies have reported the use of MWCNTs with chitosan to demonstrate antifungal properties and inhibit spore germination, radial growth and germ tube elongation [139]. Zari et al. conducted a study to demonstrate the antifungal effect against *A. niger, A. fumigatus, Candida albicans, P. chrysogenum, S. cerevisiae, F. culmorum, M. canis, T. mentagrophytes, T. rubrum, and P. lilacinum* [140]. Single-walled carbon nanotubes dispersed in tetra-arylbimesityl derivative activated with a carboxy group were used to demonstrate antifungal activity against *E. coli, S. aureus, and Candida albicans* [141].

5.4. CNTs for wastewater treatment

The potential application of CNTs has been widely studied in environmental remediation [142]. Numerous studies have highlighted the supercilious properties such as controlled surface chemistry, higher porosity, and sturdy chemical and physical interaction. This allows the CNTs as suitable candidates as an adsorbent for removing organic and inorganic pollutants from wastewater [143]. Mentioned properties qualify the CNTs as a better candidate when compared to AC and corresponding carbon-derived adsorbents [144]. Morphology of the CNTs surface and the presence of a suitable functional group in organic pollutants have been proved to be significant factors for the affinity of CNTs towards contaminants [145]. Thus, enhancing adsorption capacities.

Yang et al. conducted a study on PAHs removal from wastewater using SWCNTs and MWCNTs. Wu et al. investigated the adsorption of 22 nonpolar and polar aromatic compounds onto 10 CNTs with different diameters and lengths. The study showed the positive correlation of CNTs adsorption affinity on the basis of their mesoporous surfaces to the properties of the contaminants in contact [146]. Kah et al. studied the modelling of PAHs adsorption onto CNTs. The findings showed that the high adsorption capacity was achieved for both high and low concentrations of the PAHs, which can be attributed to the high surface area of the CNTs (200–500 m^2/g) [147].

Zhang et al. explored the PHE removal using CNTs which are magnetically modified. Increased removal efficiency, ease of regeneration, and reusability of the adsorbents were observed due to the magnetization of the CNTs [148]. Gotovac et al. measured the PHE removal from the organic solvent using SWCNTs. Non-linear nature and it is non-ionic and hydrophobic nature take it possible for PHE molecules to interact on the SWCNT surface through π–π interactions [149].

A study by Apul et al. observed a positive correlation between the CNTs outer diameter and normalized surface area for PHE adsorption. The reduction in surface curvature as a result of increasing CNT diameter caused the PHE molecules to align with the absorbents [150]. Thus, CNTs play a critical role in wastewater cleaning. The enormous potential of CNTs as adsorbent for more efficient wastewater treatment necessitates more research and development for scale-up.

5.5. CNT in electromagnetic wave absorption

In recent years, CNTs have been widely used for electromagnetic wave absorption (EMW) due to their excellent electrical properties, low density, flexibility, and large surface area. Yue et al. developed the bamboo-shaped hybrid carbon nanotube (CNT/MXene) at ultra-low temperature to enhance the electro wave absorption properties. Results indicated that CNT/MXene had batter EMW adsorption properties compared to the Mxene. The maximum EMW absorption capacity was achieved at a thickness of 2.5 mm with a minimum reflection loss (RL_{min}) of −52.56 dB and effective bandwidth (EBW) of 2.16 GHz [151]. Li et al. manufactured the Ti_3C_2X/CNT nanocomposite through a simple CVD method to enhance the electromagnetic wave absorption properties. Findings show that the EAW is up to 4.46 GHz with a thickness of only 1.55 mm, and RL_{min} value reaches -52.9 dB at 7.15 GHz with a thickness of 2.65 mm [152].

Zhao et al. produced amorphous CNTs (ACNT), and lanthanum nitrate dopped ACNT in arc discharge furnace at 600 °C in presence of Co–Ni alloy powders catalysts. The results revealed that the EMW adsorption characteristics of ACNTs are excellent to multi-walled CNT and significantly enhanced by doping 6 wt % lanthanum nitrates. The RL_{min} value of a lanthanum nitrate doped ACNT/PVC composite was −25.02 dB at 14.44 GHz [153]. Tian et al. have developed the carbon nitride nanotubes/cobalt composite at 700 °C with a heating rate of 2 °C/min. The findings shows that the RLmin value of −63.90 dB was obtained at a thickness of 1.96 mm, and the EAB ($RL \leq -10$ dB) attained 4.44 GHz at an ultra-thin thickness of 1.51 mm [154].

5.6. CNTs used as a catalyst

CNTs have become a distinctive carbon allotrope with fascinating catalytic potential. Their primary application is as support for inorganic metal catalysts, such as molecular catalysts, metal nanoparticles, metal oxides, or even more sophisticated hierarchical hybrids [155]. Mestl et al. performed the oxidative dehydrogenation of ethylbenzene to styrene in the presence of a different catalysts (CNTs, graphite, and soot). The 37 % higher specific yield in styrene demonstrated the advantage of CNTs [156]. Moreover, CNTs can used in electrocatalytic reactions. Both the N and p-doped MWCNTs exhibit good activity toward the oxygen reduction reaction; the former does so by way of an effective four-electron process in the alkaline condition, while the latter does so by way of a two-electron process [157].

In addition to electrolytic catalysis, N-doped SWCNTs and MWCNTs can also be used as normal liquid phase organic catalysis. For instance, the aerobic oxidation of cyclohexane to produce adipic acid and its precursors cyclohexanol and cyclohexanone using N-doped CNTs was successful [158]. The adaptability and competitiveness of the o, f and p -CNTs as metal-free catalysts is unsurpassed by any other catalyst.

In addition there are also other application in of CNTs such as in making nano emitters, in biogas production, nano-sensors, different type of batteries, supercapacitors, additives in phase change materials, nanofluids [159, 160, 161, 162, 163].

6. Knowledge gap and future aspects

- There are several methods for the synthesis of CNTs, such as Arc discharge, Laser ablation, CVD, PECVD, Flame pyrolysis, liquid pyrolysis and microwave irradiation. However, CNTs growth in a few minutes and at low temperature can be achieved by microwave heating. Hence, in order to be able to fully exploit this technique, further research and development are required.
- Different carbon precursors are used for the synthesis of the CNTs, such as carbon fibre, graphite, graphene, reduced graphene oxides, ferrocene, biomass and biochar in the microwave irradiation techniques. The development of CNTs using biochar as precursor through microwave irradiation is not widely studied by researchers. Therefore, more research is required to know the potential of these precursors.
- The growth mechanism of CNTs through microwave irradiation is complex and not fully understood. The mechanism of formation of CNTs using biochar is not fully studied. As a result, additional study is needed to obtain a fundamental understanding of the mechanism of CNTs growth and to change the molecular structure of biochar into CNTs under microwave radiation.
- The optimization of scale-up parameters of CNTs growth under microwave irradiation is not widely studied by researchers. However, more research and development is needed to make the most of this process.
- CNTs properties mostly depend on the precursor, catalyst and method used for synthesis. Hence, an in-depth research is needed in the optimization of the properties of CNTs. The kinetics and thermodynamics of development must also be fully understood in order to be able to manage the morphology, size, uniformity, and orientation of CNTs to attain better and distinctive features.
- It is still challenging to synthesize the CNTs without defects and impurities (catalysts nanoparticles encapsulated inside the CNTs), which restricts their use and commercialization. More research is required to produce CNTs with no structural flaws and impurities.
- A morphological investigation of the CNTs becomes a very tedious and time-consuming process due to the miniature size of CNTs and small sample size. In order to provide a qualitative and quantitative assessment of the prepared CNT structure, kinds of defects, defect density, growth rate, and evaluation of CNT geometry, there is a strong need for image processing software and quantitative models which can easily find out these properties.
- CNTs widely used in applications such as wastewater treatment, nano metal oxide composites, biomedical sector, energy and storage devices by the researcher at a low level or at a lab scale. Therefore, in the scale-up of these potential applications, research and development are required.

7. Conclusion

In this article, the authors thoroughly covered the previously and recently developed CNTs synthesis processes and their characterization and applications. To date, a number of synthesis methods have been developed for fast and low-temperature CNTs growth. In addition, the cost and bulk production of CNTs had a significant impact on commercialization. Several techniques are available for synthesising CNTs, among which Arc Discharge, Laser ablation, and CVD have been widely used. The CVD method is used primarily for the bulk production of CNTs that operate at high temperatures. CNTs were created at high temperatures (over 1700 °C) from the graphite electrode using the Arc – discharge process. This method is also used for large production SWCNTs/MWCNTs. However, the encapsulation of metal catalysts (Fe, Co, Ni) in CNTs would require additional purifying stages, resulting in a limited yield of CNTs. Laser ablation is similar to the Arc-discharge technique, and it requires high voltage and temperature.

In the present study, microwave irradiation methods opted in the last decade for the CNTs growth have been reviewed. In this technique, CNTs growth can be achieved at a lower temperature (less than 500 °C), require less synthesis time (less than 5 min), and are economical compared to other techniques. Additionally, higher carbon order of CNTs was achieved due to increment in aromatic rings cluster during microwave heating.

CNTs have a wide range of applications, such in the biomedical sector, energy conversion and storage devices, nanocomposites, catalysts, electromagnetic wave absorption, PAH adsorption from industrially contaminated water, etc. It was observed that flexibility and work function increased with the introduction of CNTs in the transparent conducting films. Moreover, physical properties such as electrical conductivity, electron mobility, thermal conductivity, resistivity, etc., were increased by applying CNTs as nanocomposites in nanodevices. In environmental remediation, CNTs have been widely used in recent times. Due to controlled surface chemistry and higher porosity, CNTs can be used as adsorbents for the removal of organic and inorganic pollutants from aqua.

Because of their superior electrical and mechanical properties, the discovery of synthesis techniques for large-scale mass manufacturing of CNTs is extremely desirable. CNTs have the potential to transform science and engineering around the world in areas such as biosensors, hydrogen storage, Li-ion batteries, nano electrical devices, and composite materials.

Declarations

Author contribution statement

Paramjeet Baghel: Conceptualization, Methodology Investigation, Writing – original draft Writing – Review & Editing; Anil Kumar Sakhiya: Writing – original draft; Priyanka Kaushal: Resources and overall supervision.

Funding statement

This research did not receive any specific grant from funding agencies in the public, commercial, or not-for-profit sectors.

Data availability statement

Data will be made available on request.

Declaration of interest's statement

The authors declare no conflict of interest.

Additional information

No additional information is available for this paper.

Acknowledgements

The authors appreciatively acknowledge the financial and experimental support from Centre for Rural Development and Technology. The authors thank Ms Shivangi Pathak for constructive suggestions in preparing the manuscript.

References

[1] S. Iijima, Helical microtubules of graphitic carbon, Nature 354 (6348) (1991) 56–58.
[2] S. Iijima, T. Ichihashi, Single-shell carbon nanotubes of 1-nm diameter, Nature 363 (6430) (1993) 603–605.
[3] D.S. Bethune, et al., Cobalt-catalysed growth of carbon nanotubes with single-atomic-layer walls, Nature 363 (6430) (1993) 605–607.
[4] M.S. Dresselhaus, G. Dresselhaus, P.C. Eklund, A.M. Rao, Carbon Nanotubes, 2000, pp. 331–379.
[5] F. Liu, R.M. Wagterveld, B. Gebben, M.J. Otto, P.M. Biesheuvel, H.V.M. Hamelers, Carbon nanotube yarns as strong flexible conductive capacitive electrodes, Colloids and Interface Science Communications 3 (2014) 9–12.
[6] T. Yamada, et al., A stretchable carbon nanotube strain sensor for human-motion detection, Nat. Nanotechnol. 6 (5) (Mar. 2011) 296–301.
[7] J.M. Schnorr, T.M. Swager, Emerging applications of carbon nanotubes, Chem. Mater. 23 (3) (2011) 646–657. American Chemical Society.
[8] M.F.L. de Volder, S.H. Tawfick, R.H. Baughman, A.J. Hart, Carbon nanotubes: present and future commercial applications, Science 339 (2013) 535–539. American Association for the Advancement of Science.
[9] E. Pop, D. Mann, Q. Wang, K. Goodson, H. Dai, Thermal conductance of an individual single-wall carbon nanotube above room temperature, Nano Lett. 6 (1) (Jan. 2006) 96–100.
[10] P. Avouris, Z. Chen, V. Perebeinos, Carbon-based electronics, Nat. Nanotechnol. 2 (10) (2007) 605–615. Nature Publishing Group.
[11] M.H. Rüummeli, P. Ayala, T. Pichler, Carbon nanotubes and related structures: production and formation, in: Carbon Nanotubes and Related Structures: Synthesis, Characterization, Functionalization, and Applications, 2010.
[12] P. Hildago-Oporto, R. Navia, R. Hunter, G. Coronado, M.E. Gonzalez, Synthesis of carbon nanotubes using biochar as precursor material under microwave irradiation, J. Environ. Manag. 244 (2019) 83–91.
[13] P. Baghel, P. Kaushal, Rapid synthesis of carbon nanotubes from Prosopis Juliflora biochar using microwave irradiation, Mater. Sci. Eng., B 286 (2022) 115987.
[14] A.F. Ismail, P.S. Goh, J.C. Tee, S.M. Sanip, M. Aziz, A review of purification techniques for carbon nanotubes, Nano 3 (03) (2008) 127–143.
[15] P. Baghel, A.K. Sakhiya, P. Kaushal, Influence of temperature on slow pyrolysis of Prosopis Juliflora: an experimental and thermodynamic approach, Renew. Energy 185 (Feb. 2022) 538–551.
[16] A.K. Sakhiya, A. Anand, P. Kaushal, Production, activation, and applications of biochar in recent times, Biochar 2 (3) (2020) 253–285.
[17] A.K. Sakhiya, P. Baghel, A. Anand, V.K. Vijay, P. Kaushal, A comparative study of physical and chemical activation of rice straw derived biochar to enhance Zn+2 adsorption, Bioresour Technol Rep 15 (2021) 100774.
[18] L.S. Ying, M.A. bin Mohd Salleh, H.B. Mohamed Yusoff, S.B. Abdul Rashid, J.B. Abd. Razak, Continuous production of carbon nanotubes - a review, J. Ind. Eng. Chem. 17 (3) (2011) 367–376.
[19] V.G. Pol, P. Thiyagarajan, Remediating plastic waste into carbon nanotubes, J. Environ. Monit. 12 (2) (2010) 455–459.
[20] S. I.- Nature and Undefined, Synthesis of Carbon Nanotubes, 1991.
[21] Y. Ando, X. Zhao, T. Sugai, M. Kumar, Growing carbon nanotubes, Mater. Today 7 (10) (2004) 22–29.
[22] T.W. Ebbesen, P.M. Ajayan, Large-scale synthesis of carbon nanotubes, Nature 358 (6383) (1992) 220–222.
[23] D.S. Bethune, et al., Cobalt-catalysed growth of carbon nanotubes with single-atomic-layer walls, Nature 363 (6430) (1993) 605–607.
[24] S. Iijima, T. Ichihashi, Single-shell carbon nanotubes of 1-nm diameter, Nature 363 (6430) (1993) 603–605.
[25] R. Saito, G. Dresselhaus, M.S. Dresselhaus, Physical Properties of Carbon Nanotubes, 1998.
[26] J. Ma, J.N. Wang, C.J. Tsai, R. Nussinov, B. Ma, Diameters of Single-Walled Carbon Nanotubes (SWCNTs) and Related Nanochemistry and Nanobiology," *Signal, Image And Video Processing*, 2010.
[27] K. Tanaka, S. Iijima, Carbon Nanotubes and Graphene 2, 2014.
[28] R.S. Wagner, W.C. Ellis, Vapor-liquid-solid mechanism of single crystal growth, Appl. Phys. Lett. 4 (5) (1964) 89–90.
[29] M.H. Rümmeli, et al., Synthesis of carbon nanotubes with and without catalyst particles, Nanoscale Res. Lett. 6 (1) (2011) 1–9.
[30] J. Lu, J. Miao, Growth mechanism of carbon nanotubes: a nano Czochralski model, Nanoscale Res. Lett. 7 (1) (2012) 1–5.
[31] J. Zhang, A. Tahmasebi, J.E. Omoriyekomwan, J. Yu, Production of carbon nanotubes on bio-char at low temperature via microwave-assisted CVD using Ni catalyst, Diam. Relat. Mater. 91 (2019) 98–106.
[32] T. Guo, P. Nikolaev, A. Thess, D.T. Colbert, R.E. Smalley, Catalytic growth of single-walled manotubes by laser vaporization, Chem. Phys. Lett. 243 (1–2) (1995) 49–54.
[33] A. Thess, et al., Crystalline ropes of metallic carbon nanotubes, Science 273 (5274) (1979) 483–487.
[34] J.H. Hafner, et al., Catalytic growth of single-wall carbon nanotubes from metal particles, Chem. Phys. Lett. 296 (1–2) (1998) 195–202.
[35] S. Lebedkin, et al., Single-wall Carbon Nanotubes with Diameters Approaching 6 Nm Obtained by Laser Vaporization, Carbon N Y 40 (3) (2002) 417–423.
[36] M. Asnawi, S. Azhari, M.N. Hamidon, I. Ismail, I. Helina, Synthesis of carbon nanomaterials from rice husk via microwave oven, J. Nanomater. 2018 (2018) 1–5.
[37] M. Zhan, G. Pan, Y. Wang, T. Kuang, F. Zhou, Ultrafast carbon nanotube growth by microwave irradiation, Diam. Relat. Mater. 77 (2017) 65–71.
[38] R. Kumar, et al., Synthesis of self-assembled and hierarchical palladium-CNTs-reduced graphene oxide composites for enhanced field emission properties, Mater. Des. 122 (2017) 110–117.
[39] N.A. Algadri, K. Ibrahim, Z. Hassan, M. Bououdina, Cost-effective single-step carbon nanotube synthesis using microwave oven, Mater. Res. Express 4 (8) (2017).
[40] R. Bajpai, H.D. Wagner, Fast growth of carbon nanotubes using a microwave oven, Carbon N Y 82 (2015) 327–336.
[41] Y. Kang, X. Yu, M. Kota, H.S. Park, Carbon nanotubes branched on three-dimensional, nitrogen-incorporated reduced graphene oxide/iron oxide hybrid architectures for lithium ion battery anode, J. Alloys Compd. 726 (2017) 88–94.
[42] J.E. Omoriyekomwan, A. Tahmasebi, J. Zhang, J. Yu, Mechanistic study on direct synthesis of carbon nanotubes from cellulose by means of microwave pyrolysis, Energy Convers. Manag. 192 (2019) 88–89.
[43] W. Zheng, P.G. Zhang, J. Chen, W.B. Tian, Y.M. Zhang, Z.M. Sun, Microwave-assisted synthesis of three-dimensional MXene derived metal oxide/carbon nanotube/iron hybrids for enhanced lithium-ions storage, J. Electroanal. Chem. 835 (2018) 205–211.
[44] G. Ortega-Cervantez, R. Gómez-Aguilar, G. Rueda-Morales, J. Ortiz-López, Microwave-assisted synthesis of sponge-like carbon nanotube arrays and their application in organic transistor devices, J. Mater. Sci. Mater. Electron. 27 (12) (2016) 12642–12648.
[45] H. Xie, et al., Microwave-assisted fabrication of carbon nanotubes decorated polymeric nano-medical platforms for simultaneous drug delivery and magnetic resonance imaging, RSC Adv. 4 (11) (2014) 5649–5652.
[46] V. Sridhar, I. Lee, H.H. Chun, H. Park, Microwave synthesis of nitrogen-doped carbon nanotubes anchored on graphene substrates, Carbon N Y 87 (2015) 186–192.
[47] S. Vadahanambi, J.H. Jung, I.K. Oh, Microwave Syntheses of Graphene and Graphene Decorated with Metal Nanoparticles, Carbon N Y 49 (13) (2011) 4449–4457.
[48] V. Sridhar, H. Park, Zeolitic imidazolate frameworks as novel precursors for microwave synthesis of carbon nanotubes, J. Alloys Compd. 781 (2019) 166–173.
[49] A. Hazarika, B.K. Deka, D. Kim, K. Kong, Y. bin Park, H.W. Park, Microwave-synthesized freestanding iron-carbon nanotubes on polyester composites of woven Kevlar fibre and silver nanoparticle-decorated graphene, Sci. Rep. 7 (2017) 1–11.
[50] S. Guo, Q. Dai, Z. Wang, H. Yao, Rapid microwave irradiation synthesis of carbon nanotubes on graphite surface and its application on asphalt reinforcement, Compos. B Eng. 124 (2017) 134–143.
[51] E.A. Burakova, et al., Novel and economic method of carbon nanotubes synthesis on a nickel magnesium oxide catalyst using microwave radiation, J. Mol. Liq. 253 (2018) 340–346.
[52] M. Ahmad, S.R.P. Silva, Low temperature growth of carbon nanotubes – a review, Carbon N Y 158 (Mar. 2020) 24–44.
[53] G. Kucukayan, et al., An experimental and theoretical examination of the effect of sulfur on the pyrolytically grown carbon nanotubes from sucrose-based solid state precursors, Carbon N Y 49 (2) (Feb. 2011) 508–517.
[54] H. Omachi, S. Matsuura, Y. Segawa, K. Itami, A modular and size-selective synthesis of [n]Cycloparaphenylenes: a step toward the selective synthesis of [n,n] single-walled carbon nanotubes, Angew. Chem. Int. Ed. 49 (52) (2010) 10202–10205.
[55] F. Liu, et al., Preparation of short carbon nanotubes by mechanical ball milling and their hydrogen adsorption behavior, Carbon N Y 41 (13) (2003) 2527–2532, Jan.
[56] G. Sun, X. Wang, P. Chen, Microfiber devices based on carbon materials, Mater. Today 18 (4) (May 2015) 215–226.
[57] Y. Gogotsi, J.A. Libera, M. Yoshimura, Hydrothermal synthesis of multiwall carbon nanotubes, J. Mater. Res. 15 (12) (2011) 2591–2594.
[58] G.Z. Chen, X. Fan, A. Luget, M.S.P. Shaffer, D.J. Fray, A.H. Windle, Electrolytic conversion of graphite to carbon nanotubes in fused salts, J. Electroanal. Chem. 446 (1–2) (1998) 1–6.
[59] M. Endo, H. Muramatsu, T. Hayashi, Y.A. Kim, M. Terrones, M.S. Dresselhaus, 'Buckypaper' from coaxial nanotubes, Nature 433 (7025) (2005) 476.
[60] M. Yilmaz, S. Raina, S.H. Hsu, W.P. Kang, Growing micropatterned CNT arrays on aluminum substrates using hot-filament CVD process, Mater. Lett. 209 (2017) 376–378.

[61] J. Lin, Y. Yang, H. Zhang, F. Li, G. Huang, C. Wu, Preparation of CNT–Co@TiB2 by catalytic CVD: effects of synthesis temperature and growth time, Diam. Relat. Mater. 106 (2020) 107830.
[62] Z. Liu, et al., Poptube approach for ultrafast carbon nanotube growth, Chem. Commun. 47 (35) (2011) 9912–9914.
[63] W. Campos Guaglianoni, A.P. Garcia, T.M. Basegio, M.A. Arcari Bassani, S. Arcaro, C. Pérez Bergmann, Influence of CVD parameters on Co-TiO2/CNT properties: a route to enhance energy harvesting from sunlight, Int. J. Appl. Ceram. Technol. 18 (4) (2021) 1297–1306, Jul.
[64] R.K. Singh, B. Ruj, A.K. Sadhukhan, P. Gupta, Conventional Pyrolysis of Plastic Waste for Product Recovery and Utilization of Pyrolytic Gases for Carbon Nanotubes Production, Environmental Science and Pollution Research, 2020, pp. 1–10.
[65] A. Tepale-Cortés, H. Moreno-Saavedra, C. Hernandez-Tenorio, T. Rojas-Ramírez, J. Illescas, Multi-walled carbon nanotubes synthesis by arc discharge method in a glass chamber, J Mex Chem Soc 65 (4) (Sep. 2021) 480–490.
[66] M. Hong, et al., Scalable synthesis of γ-Fe2O3/CNT composite as high-performance anode material for lithium-ion batteries, J. Alloys Compd. 770 (Jan. 2019) 116–124.
[67] J. Kennedy, et al., Synthesis and enhanced field emission of zinc oxide incorporated carbon nanotubes, Diam. Relat. Mater. 71 (Jan. 2017) 79–84.
[68] T. Sagara, S. Kurumi, K. Suzuki, Growth of linear Ni-filled carbon nanotubes by local arc discharge in liquid ethanol, Appl. Surf. Sci. 292 (2014) 39–43.
[69] J. Zhao, Y. Su, Z. Yang, L. Wei, Y. Wang, Y. Zhang, Arc synthesis of double-walled carbon nanotubes in low pressure air and their superior field emission properties, Carbon N Y 58 (2013) 92–98.
[70] E. Muñoz, et al., Gas and pressure effects on the production of single-walled carbon nanotubes by laser ablation, Carbon N Y 38 (10) (2000) 1445–1451.
[71] M. Kusaba, Y. Tsunawaki, Production of single-wall carbon nanotubes by a XeCl excimer laser ablation, Thin Solid Films 506 (507) (2006) 255–258.
[72] D.M. Yoon, B.J. Yoon, K.H. Lee, H.S. Kim, C.G. Park, Synthesis of carbon nanotubes from solid carbon sources by direct microwave irradiation, Carbon N Y 44 (7) (2006) 1339–1343.
[73] H. Nie, M. Cui, T.P. Russell, A Route to Rapid Carbon Nanotube Growth †, 2013, pp. 5159–5161.
[74] W. Zheng, P. Zhang, J. Chen, W.B. Tian, Y.M. Zhang, Z.M. Sun, In situ synthesis of CNTs@Ti3C2 hybrid structures by microwave irradiation for high-performance anodes in lithium ion batteries, J Mater Chem A Mater 6 (8) (2018) 3543–3551.
[75] S.K.S. Park, K. Choi, S.H. Lee, I.K. Oh, S.K.S. Park, H.S. Park, CNT branching of three-dimensional steam-activated graphene hybrid frameworks for excellent rate and cyclic capabilities to store lithium ions, Carbon N Y 116 (2017) 500–509.
[76] L. Reinert, M. Zeiger, S. Suárez, V. Presser, F. Mücklich, Dispersion analysis of carbon nanotubes, carbon onions, and nanodiamonds for their application as reinforcement phase in nickel metal matrix composites, RSC Adv. 5 (115) (2015) 95149–95159.
[77] H. Xu, et al., Characterization of multiwalled carbon nanotubes dispersing in water and association with biological effects, J. Nanomater. 2011 (2011) 938491.
[78] Y. Wang, M. Mortimer, C.H. Chang, P.A. Holden, Alginic Acid-Aided Dispersion of Carbon Nanotubes, Graphene, and boron Nitride Nanomaterials for Microbial Toxicity Testing, Nanomaterials 8 (2) (2018) 76.
[79] B. Smith, et al., Colloidal properties of aqueous suspensions of acid-treated, multi-walled carbon nanotubes, Environ. Sci. Technol. 43 (3) (2009) 819–825.
[80] W. Rashmi, et al., Stability and thermal conductivity enhancement of carbon nanotube nanofluid using gum Arabic, J. Exp. Nanosci. 6 (6) (2011) 567–579.
[81] J. Njuguna, O.A. Vanli, R. Liang, A review of spectral methods for dispersion characterization of carbon nanotubes in aqueous suspensions, Journal of Spectroscopy 2015 (2015).
[82] G.A. Rance, D.H. Marsh, R.J. Nicholas, A.N. Khlobystov, UV-vis absorption spectroscopy of carbon nanotubes: relationship between the π-electron plasmon and nanotube diameter, Chem. Phys. Lett. 493 (1–3) (2010) 19–23.
[83] H.A. Zeinabad, A. Zarrabian, A.A. Saboury, A.M.O. Alizadeh, M. Falahati, Interaction of single and multi wall carbon nanotubes with the biological systems: tau protein and PC12 cells as targets, Sci. Rep. 6 (1) (2016) 1–23.
[84] N. Khalilzadeh, et al., Single step thermal treatment synthesis and characterization of lithium tetraborate nanophosphor, J. Mater. Res. Technol. 5 (1) (2016) 37–44.
[85] P.G. Collins, M.S. Arnold, P. Avouris, Engineering carbon nanotubes and nanotube circuits using electrical breakdown, Science (1979) 2001.
[86] M.S. Dresselhaus, P.C. Eklund, Phonons in carbon nanotubes, Adv. Phys. (2000).
[87] M.S. Dresselhaus, G. Dresselhaus, R. Saito, A. Jorio, Raman spectroscopy of carbon nanotubes, Phys. Rep. 409 (2) (2005) 47–99.
[88] R. Saito, A. Jorio, J. Jiang, K. Sasaki, G. Dresselhaus, M.S. Dresselhaus, Optical Properties of Carbon Nanotubes and Nanographene, in: Oxford Handbook of Nanoscience and Technology, 2, 2010. Materials: Structures, Properties and Characterization Techniques.
[89] L.G. Cançado, et al., Quantifying defects in graphene via Raman spectroscopy at different excitation energies, Nano Lett. 11 (8) (2011) 3190–3196.
[90] A.C. Ferrari, Raman spectroscopy of graphene and graphite: disorder, electron-phonon coupling, doping and nonadiabatic effects, Solid State Commun. 143 (1–2) (2007) 47–57.
[91] G. Moraitis, Z. Špitalský, F. Ravani, A. Siokou, C. Galiotis, Electrochemical Oxidation of Multi-wall Carbon Nanotubes, Carbon N Y 49 (8) (2011) 2702–2708.
[92] N. Kure, et al., Simple microwave-assisted synthesis of carbon nanotubes using polyethylene as carbon precursor, J. Nanomater. 2017 (2017).
[93] D.C.D. Nath, V. Sahajwalla, Application of fly ash as a catalyst for synthesis of carbon nanotube ribbons, J. Hazard Mater. 192 (2) (2011) 691–697.
[94] H. Jantoljak, J.P. Salvetat, L. Forró, C. Thomsen, Low-energy Raman-active phonons of multiwalled carbon nanotubes, Appl. Phys. A 67 (1) (1998) 113–116.
[95] S. Arepalli, et al., Protocol for the Characterization of Single-wall Carbon Nanotube Material Quality, Carbon N Y (2004).
[96] W.E. Alvarez, B. Kitiyanan, A. Borgna, D.E. Resasco, Synergism of Co and Mo in the Catalytic Production of Single-wall Carbon Nanotubes by Decomposition of CO, Carbon N Y (2001).
[97] H. Zhu, et al., Hydrogen adsorption in bundles of well-aligned carbon nanotubes at room temperature, Appl. Surf. Sci. 178 (1–4) (2001) 50–55.
[98] B.J. Yoon, et al., Fabrication of flexible carbon nanotube field emitter arrays by direct microwave irradiation on organic polymer substrate, J. Am. Chem. Soc. 127 (23) (2005) 8234–8235.
[99] J.I. Goldstein, et al., SEM image interpretation, in: Scanning Electron Microscopy and X-Ray Microanalysis, 2018.
[100] I.M. Watt, The Principles and Practice of Electron Microscopy, 1997.
[101] P.D. Nellist, Scanning Transmission Electron Microscopy, Springer Handbooks, 2019.
[102] M. Vizuete, et al., Photochemical evidence of electronic interwall communication in double-wall carbon nanotubes, Chem. Eur J. 18 (52) (2012) 16922–16930.
[103] H. Chen, et al., Broad-spectrum antibacterial activity of carbon nanotubes to human gut bacteria, Small 9 (16) (2013) 2735–2746.
[104] L. Chen, H. Liu, K. Yang, J. Wang, X. Wang, The effect of reaction temperature on the diameter distribution of carbon nanotubes grown from ethylene decomposition over a Co-La-O catalyst, Mater. Chem. Phys. 112 (2) (2008) 407–411.
[105] D. Eder, Carbon nanotube-inorganic hybrids, Chem. Rev. 110 (3) (2010) 1348–1385.
[106] P.C. Ma, N.A. Siddiqui, G. Marom, J.K. Kim, Dispersion and functionalization of carbon nanotubes for polymer-based nanocomposites: a review, Compos. Appl. Sci. Manuf. 41 (10) (2010).
[107] G. Yamamoto, et al., Nanotube fracture during the failure of carbon nanotube/alumina composites, Carbon N Y 49 (12) (2011) 3709–3716.
[108] G. Yamamoto, M. Omori, T. Hashida, H. Kimura, A novel structure for carbon nanotube reinforced alumina composites with improved mechanical properties, Nanotechnology 19 (31) (2008) 315708.
[109] H. Wei, et al., Regenerable granular carbon nanotubes/alumina hybrid adsorbents for diclofenac sodium and carbamazepine removal from aqueous solution, Water Res. 47 (12) (2013) 4139–4147.
[110] A.K. Keshri, J. Huang, V. Singh, W. Choi, S. Seal, A. Agarwal, Synthesis of aluminum oxide coating with carbon nanotube reinforcement produced by chemical vapor deposition for improved fracture and wear resistance, Carbon N Y 48 (2) (2010) 431–442.
[111] M. Malakootian, H.J. Mansoorian, A. Hosseini, N. Khanjani, Evaluating the efficacy of alumina/carbon nanotube hybrid adsorbents in removing Azo Reactive Red 198 and Blue 19 dyes from aqueous solutions, Process Saf. Environ. Protect. 96 (2015) 125–137.
[112] S. Sharma, S. Hussain, K. Sengupta, S.S. Islam, Development of MWCNTs/alumina composite-based sensor for trace level ammonia gas sensing, Appl. Phys. Mater. Sci. Process 111 (3) (2013) 965–974.
[113] P. Liu, Y. Guo, Q. Xu, F. Wang, Y. Li, K. Shao, Enhanced photocatalytic performance of ZnO/multi-walled carbon nanotube nanocomposites for dye degradation, Ceram. Int. 40 (4) (2014) 5629–5633.
[114] G. Kaur, N.V. Pulagara, R. Kumar, I. Lahiri, Metal foam-carbon nanotube-reduced graphene oxide hierarchical structures for efficient field emission, Diam. Relat. Mater. 106 (2020) 107847.
[115] N.M. Hung, et al., Carbon nanotube-metal oxide nanocomposite gas sensing mechanism assessed via NO2 adsorption on n-WO3/p-MWCNT nanocomposites, Ceram. Int. 46 (18) (2020) 29233–29243.
[116] Y. Yan, X. Bo, L. Guo, MOF-818 metal-organic framework-reduced graphene oxide/multiwalled carbon nanotubes composite for electrochemical sensitive detection of phenolic acids, Talanta 218 (2020) 121123.
[117] R.H. Baughman, A.A. Zakhidov, W.A. de Heer, Carbon nanotubes - the route toward applications, Science 297 (5582) (2002) 787–792.
[118] M.G. Helander, et al., Chlorinated indium tin oxide electrodes with high work function for organic device compatibility, Science (1979) 2011.
[119] E.M. Doherty, et al., The spatial uniformity and electromechanical stability of transparent, conductive films of single walled nanotubes, Carbon N Y 47 (10) (2009) 2466–2473.
[120] K.H. Ok, et al., Ultra-thin and smooth transparent electrode for flexible and leakage-free organic light-emitting diodes, Sci. Rep. 5 (1) (2015) 1–8.
[121] N. Ferrer-Anglada, J. Pérez-Puigdemont, J. Figueras, M.Z. Iqbal, S. Roth, Flexible, transparent electrodes using carbon nanotubes, Nanoscale Res. Lett. 7 (1) (2012) 571.
[122] D.S. Hecht, L. Hu, G. Irvin, Emerging transparent electrodes based on thin films of carbon nanotubes, graphene, and metallic nanostructures, Adv. Mater. 23 (13) (2011) 1482–1513.
[123] L. Hu, D.S. Hecht, G. Grüner, Carbon nanotube thin films: fabrication, properties, and applications, Chem. Rev. 110 (10) (2010) 5790–5844.
[124] R. Xiang, et al., Spray coating as a simple method to prepare catalyst for growth of diameter-tunable single-walled carbon nanotubes, Carbon 64 (2013) 537–540.
[125] N. Saran, K. Parikh, D.S. Suh, E. Muñoz, H. Kolla, S.K. Manohar, Fabrication and characterization of thin films of single-walled carbon nanotube bundles on flexible plastic substrates, J. Am. Chem. Soc. 126 (14) (2004) 4462–4463.
[126] D. Janas, K.K. Koziol, A review of production methods of carbon nanotube and graphene thin films for electrothermal applications, Nanoscale 6 (6) (2014) 3037–3045.

[127] X. Li, et al., Langmuir-Blodgett assembly of densely aligned single-walled carbon nanotubes from bulk materials, J. Am. Chem. Soc. 129 (16) (2007) 4890–4891.
[128] A. Kaskela, et al., Aerosol-synthesized SWCNT networks with tunable conductivity and transparency by a dry transfer technique, Nano Lett. 10 (11) (2010) 4349–4355.
[129] C. Revathi, K. Rajavel, M. Saranya, R.T.R. Kumar, MWCNT based non-enzymatic H 2 O 2 sensor: influence of amine functionalization on the electrochemical H 2 O 2 sensing, J. Electrochem. Soc. 163 (13) (2016) B627–B632.
[130] J. Wang, Y. Wang, Z. Yao, C. Liu, Y. Xu, Z. Jiang, Preparation of Fe3O4/MWCNT nano-hybrid and its application as phenol sensor, Mater. Res. Express 5 (7) (2018), 075003.
[131] R. Ramalingame, et al., Flexible piezoresistive sensor matrix based on a carbon nanotube PDMS composite for dynamic pressure distribution measurement, Journal of Sensors and Sensor Systems 8 (1) (2019) 1–7.
[132] A. Ali, A. Khan, K.S. Karimov, A. Ali, A. Daud Khan, Pressure sensitive sensors based on carbon nanotubes, graphene, and its composites, J. Nanomater. 2018 (2018).
[133] C. Song, et al., A shape memory high-voltage supercapacitor with asymmetric organic electrolytes for driving an integrated NO2 gas sensor, Adv. Funct. Mater. 29 (24) (2019) 1901996.
[134] A. Seyfoori, S. Sarfarazijami, S.A. Seyyed Ebrahimi, pH-responsive carbon nanotube-based hybrid nanogels as the smart anticancer drug carrier, Artif Cells Nanomed Biotechnol 47 (1) (2019 Dec) 1437–1443, 1596939.
[135] J.T.W. Wang, et al., The relationship between the diameter of chemically-functionalized multi-walled carbon nanotubes and their organ biodistribution profiles in vivo, Biomaterials 35 (35) (2014) 9517–9528.
[136] S. Wen, H. Liu, H. Cai, M. Shen, X. Shi, Targeted and pH-responsive delivery of doxorubicin to cancer cells using multifunctional dendrimer-modified multi-walled carbon nanotubes, Adv Healthc Mater 2 (9) (2013) 1267–1276.
[137] A.O. Oyelami, K.T. Semple, Impact of carbon nanomaterials on microbial activity in soil, Soil Biol. Biochem. 86 (2015) 172–180.
[138] P. Jackson, et al., Bioaccumulation and ecotoxicity of carbon nanotubes, Chem. Cent. J. 7 (1) (2013) 1–21.
[139] A. el Ghaouth, J. Arul, A. Asselin, N. Benhamou, Antifungal activity of chitosan on post-harvest pathogens: induction of morphological and cytological alterations in Rhizopus stolonifer, Mycol. Res. 96 (9) (1992) 769–779.
[140] H. Zare-Zardini, A. Amiri, M. Shanbedi, M. Memarpoor-Yazdi, A. Asoodeh, Studying of antifungal activity of functionalized multiwalled carbon nanotubes by microwave-assisted technique, Surf. Interface Anal. 45 (3) (2013) 751–755.
[141] E.L. Ursu, et al., Aqueous dispersion of single-walled carbon nanotubes using tetra-phenyl bimesitylene derivative via noncovalent modification and improved antimicrobial activity, J. Nanosci. Nanotechnol. 19 (12) (2019) 7960–7966.
[142] W. Zhang, et al., Effects of carbon nanotubes on biodegradation of pollutants: positive or negative? Ecotoxicol. Environ. Saf. 189 (2020).
[143] S. Pathak, A.K. Sakhiya, A. Anand, K.K. Pant, P. Kaushal, A state-of-the-art review of various adsorption media employed for the removal of toxic Polycyclic aromatic hydrocarbons (PAHs): an approach towards a cleaner environment, J. Water Proc. Eng. 47 (2022) 102674.
[144] J.G. Yu, et al., Aqueous adsorption and removal of organic contaminants by carbon nanotubes, Sci. Total Environ. (1) (2014) 482–483, 241–251.
[145] T.A. Saleh, A. Sarı, M. Tuzen, Carbon nanotubes grafted with poly(trimesoyl, m-phenylenediamine) for enhanced removal of phenol, J. Environ. Manag. 252 (2019) 109660.
[146] W. Wu, et al., Correlation and prediction of adsorption capacity and affinity of aromatic compounds on carbon nanotubes, Water Res. 88 (2016) 492–501.
[147] M. Kah, X. Zhang, M.T.O. Jonker, T. Hofmann, Measuring and modeling adsorption of PAHs to carbon nanotubes over a six order of magnitude wide concentration range, Environ. Sci. Technol. 45 (14) (2011) 6011–6017.
[148] J. Zhang, R. Li, G. Ding, Y. Wang, C. Wang, Sorptive removal of phenanthrene from water by magnetic carbon nanomaterials, J. Mol. Liq. 293 (2019) 111540.
[149] S. Gotovac, C.M. Yang, Y. Hattori, K. Takahashi, H. Kanoh, K. Kaneko, Adsorption of polyaromatic hydrocarbons on single wall carbon nanotubes of different functionalities and diameters, J. Colloid Interface Sci. 314 (1) (2007) 18–24.
[150] O.G. Apul, T. Shao, S. Zhang, T. Karanfil, Impact of carbon nanotube morphology on phenanthrene adsorption, Environ. Toxicol. Chem. 31 (1) (2012) 73–78.
[151] Y. Yue, Y. Wang, X. Xu, C. Wang, Z. Yao, D. Liu, In-situ growth of bamboo-shaped carbon nanotubes and helical carbon nanofibers on Ti3C2Tx MXene at ultra-low temperature for enhanced electromagnetic wave absorption properties, Ceram. Int. 48 (5) (2022) 6338–6346.
[152] X. Li, et al., Ti3C2 MXenes modified with in situ grown carbon nanotubes for enhanced electromagnetic wave absorption properties, J Mater Chem C Mater 5 (16) (2017) 4068–4074.
[153] T. Zhao, et al., Electromagnetic Wave Absorbing Properties of Amorphous Carbon Nanotubes, Scientific Reports 4 (1) (2014) 1–7.
[154] K. Tian, et al., In-situ synthesis of graphite carbon nitride nanotubes/Cobalt@ Carbon with castor-fruit-like structure as high-efficiency electromagnetic wave absorbers, J. Colloid Interface Sci. 620 (2022) 454–464.
[155] M. Melchionna, S. Marchesan, M. Prato, P. Fornasiero, Carbon nanotubes and catalysis: the many facets of a successful marriage, Catal. Sci. Technol. 5 (8) (2015) 3859–3875.
[156] G. Mestl, N.I. Maksimova, N. Keller, V. v Roddatis, R. Schlögl, Carbon nanofilaments in heterogeneous catalysis: an industrial application for new carbon materials? Angew Chem. Int. Ed. Engl. 40 (11) (2001) 2066–2068.
[157] X. Xu, S. Jiang, Z. Hu, S. Liu, Nitrogen-doped carbon nanotubes: high electrocatalytic activity toward the oxidation of hydrogen peroxide and its application for biosensing, ACS Nano 4 (7) (2010) 4292–4298.
[158] H. Yu, et al., Selective catalysis of the aerobic oxidation of cyclohexane in the liquid phase by carbon nanotubes, Angew. Chem. Int. Ed. 50 (17) (2011) 3978–3982.
[159] D.G. Atinafu, S. Wi, B.Y. Yun, S. Kim, Engineering biochar with multiwalled carbon nanotube for efficient phase change material encapsulation and thermal energy storage, Energy 216 (2021) 119294.
[160] M.H. Ahmadi, A. Mirlohi, M. Alhuyi Nazari, R. Ghasempour, A review of thermal conductivity of various nanofluids, J. Mol. Liq. 265 (2018) 181–188.
[161] Q. Gu, J. Chen, Carbon-nanotube-based nano-emitters: a review, J. Lumin. 200 (2018) 181–188.
[162] S. Kumar, M. Nehra, D. Kedia, N. Dilbaghi, K. Tankeshwar, K.H. Kim, Carbon nanotubes: a potential material for energy conversion and storage, Prog. Energy Combust. Sci. 64 (2018) 219–253.
[163] S.A. Khan, T.C. D' Silva, S. Kumar, R. Chandra, V.K. Vijay, A. Misra, Mutually trading off biochar and biogas sectors for broadening biomethane applications: a comprehensive review, J. Clean. Prod. 318 (2021) 128593.